بسم الله الرحمن الرحيم

Islamic University of Technology (IUT)
Organization of Islamic Cooperation (OIC)
Gazipur-1704, Dhaka, Bangladesh

SMALL SIGNAL STABILITY ANALYSIS OF GRID CONNECTED PV WITH BESS

SUBMITTED BY:

Md. Imranul Hai Shuvo (142441)
Md. Shawonuzzaman (142475)
Md. Tanvir Pavel (142411)
Zarif Sultan (142478)

SUPERVISED BY:

DR. ASHIK AHMED
Associate Professor
Department Of Electrical And Electronic Engineering (EEE)

Department Of Electrical And Electronic Engineering (EEE)
Islamic University of Technology (IUT)
Organization of Islamic Cooperation (OIC)

NOVEMBER 2018

CERTIFICATE OF APPROVAL

Certified that the project dissertation entitled

"Small Signal Stability Analysis Of grid connected PV with BESS"

Is submitted to the Department of Electrical and Electronic Engineering

Islamic University of Technology

(Bangladesh)

In the partial fulfillment of the requirements
For the award of

BACHELORS OF SCIENCE IN
ELECTRICAL & ELECTROINC ENGINEERING

Supervised by:

Associate Prof. Dr. ASHIK AHMED

Thesis Advisor

Approved by:

Prof. Dr. MD. ASHRAFUL HAQUE

Head of EEE department

ACKNOWLEDGMENTS

All praise and thanks to Almighty Allah who has showered us with His invaluable blessings throughout our lives, giving us strength and spirit to complete this project.

We would like to express our deepest gratitude to our project advisor ***Dr. ASHIK AHMED.*** *Whose personal supervision, advice and valuable guidance helped us go through all the stages and complete appreciably our final year project. Without his stimulus for work and knowledge of the project idea, the completion of the project would have been impossible.*

In the end we would like to show our deepest respect to our parents, family, friends and all those who showed patience and tenacity with us to finish with success.

Contents

List of figures

LIST OF ACRONYMS

PV	Photovoltaic
BDC	Bi-directional Converter
BESS	Battery Energy Storage System
PI	Proportional Integral
VSI	Voltage Source Inverter
CSI	Current Source Inverter
MPPT	Maximum Power Point Tracking
GCPV	Grid Connected Photovoltaic

Chapter 1

Introduction

1.1 Background

Renewable energy sources have enormous potential and are capable of generating energy levels much greater than the current world demand. The use of such sources can help to reduce pollution, increase environmental sustainability, and lower the consumption of fossil fuels. Increasing climate changes, coupled with the depletion of fossil fuels, are the main driving forces for renewable energy legislation, incentives, and commercialization. The principal types of renewable energy sources include solar, wind, and hydro. Solar power is one of the most promising renewable sources, as it is more predictable than wind energy, and less vulnerable to seasonal changes as hydro power. Power generation by hydro or wind is restricted to the sites where resources are available. Solar energy can be harnessed at the point of demand both in rural and urban areas, thus decreasing the cost of transmitting the electricity (costs of transmission). Grid connected Photovoltaic (PV) systems that are connected to the distribution level, particularly with MW capacity, are increasing at an aggressive rate, in order to meet the energy demand. However, there is less experience in the interconnection of utility-scale PV systems with the distribution network, where loads are present. The Grid or also known as the utility is an interconnected network, which supplies electricity to the consumers. This interconnected network consists of resources for transmission and distribution of power or electricity from the generation station to a

distribution station, via high-voltage transmission lines. This voltage is then delivered to the customers, from the distribution stations.

Utility-scale PV systems need special attention, unlike small scale PV systems, which are limited to a few hundreds kW and are unlikely to show an impression on the distribution system. Thus, there is a need to analyze the large scale, three-phase PV systems employed as Photovoltaic Distributed Generation (PV-DGs), in terms of performance, dynamic characteristics, and control. D.M Chapin, C.S Fuller, and G.S. Person of Bell laboratory patented the solar cell, in 1954. The next year, Hoffman Electronics' semiconductor division announced the first commercial photo- voltaic product that was 2% efficient, priced at 25$ per cell, and generating power of 14 mW each. By 1980, photovoltaics began finding many off-grid applications such as pocket calculators, highway lights, and small home applications. By 2002, worldwide photovoltaic power production reached 600 MW per year, and was increasing at a rate of over 40% per year. The continued discovery and development of silicon and other photovoltaic materials have helped increase cell efficiency and decrease cost. At present, solar PV power costs less than 2$ per watt [1]. The total global solar photovoltaic capacity is fast approaching the 100 GW milestone, as per the International Energy Agency. [4] About 37 GW was connected to the grid in 2013, and almost the same amount in 2012. Europe currently represents 59% of the world PV market, but is facing competition from the Asia-Pacific Region. In 2012, China was the second-largest PV market for new installations [3], thus placing solar power generation in second position in terms of the new sources of power generation.

Solar Photovoltaic Distributed Generation (PV-DG) systems represent one of the fastest-growing types of renewable energy sources worldwide, currently being integrated into

distribution systems [2]. The most crucial aspect of the system is that the technical requirements of the utility power system need to be satisfied to ensure the safety of the PV installer and the reliability of the utility grid [5]. It is very important to understand the technical requirements when performing an interconnection between two systems. For example, critical interconnection problems such as harmonic distortion, islanding detection, and electromagnetic interference need to be identified and solved. The interconnection of PV systems with the grid is accomplished with the help of a supply electric power to electrical equipment. The inverter plays an important role in this interconnection. There is a need for the PV arrays and inverter to be characterized based on the geographical location of the PV system and the installation configuration, but also based on the defects that occur during the operation of the system [6-10]. In a grid-interconnected PV system, the inverter plays a key role, and its reliability and safety are of the utmost importance to the system. As part of the PV-DG plant interconnection impact studies, which include the typical power flow analysis, an in-depth research is required into the potentially dynamic impacts of PV-DG units on the feeder voltages under various load conditions. The investigation into the dynamic impacts of the system lead to the development of various control strategies/techniques needed for the stability and smooth operation of the PV-DG systems.

1.2. Motivation

Nowadays, renewable energy has been more and more attractive due to the severe environmental protection regulations and the shortage of conventional energy sources. Photovoltaic (PV) generation is the technique which uses photovoltaic cell to convert solar energy to electric energy.

Photovoltaic energy is assuming increasingly important as a renewable energy source because of its distinctive advantages, such as simple configuration, easy allocation, free of pollution, low maintenance cost, etc. However, the disadvantage is that photovoltaic generation is intermittent, depending upon weather conditions. Thus, energy storage element is necessary to help get stable and reliable power from PV system for loads or utility grid, and thus improve both steady and

dynamic behaviors of the whole generation system. Because of its mature technology, low cost and high efficiency, battery energy storage system (BESS) is used widely in distribution generation technology. BESS can be integrated into PV generation system to form a hybrid PV/Battery generation system, which can be more stable and reliable. An integral grid-connected PV+BESS generation system is composed of PV array, battery, power electronic converters, filters, controllers, and utility grid.

Figure 1.1

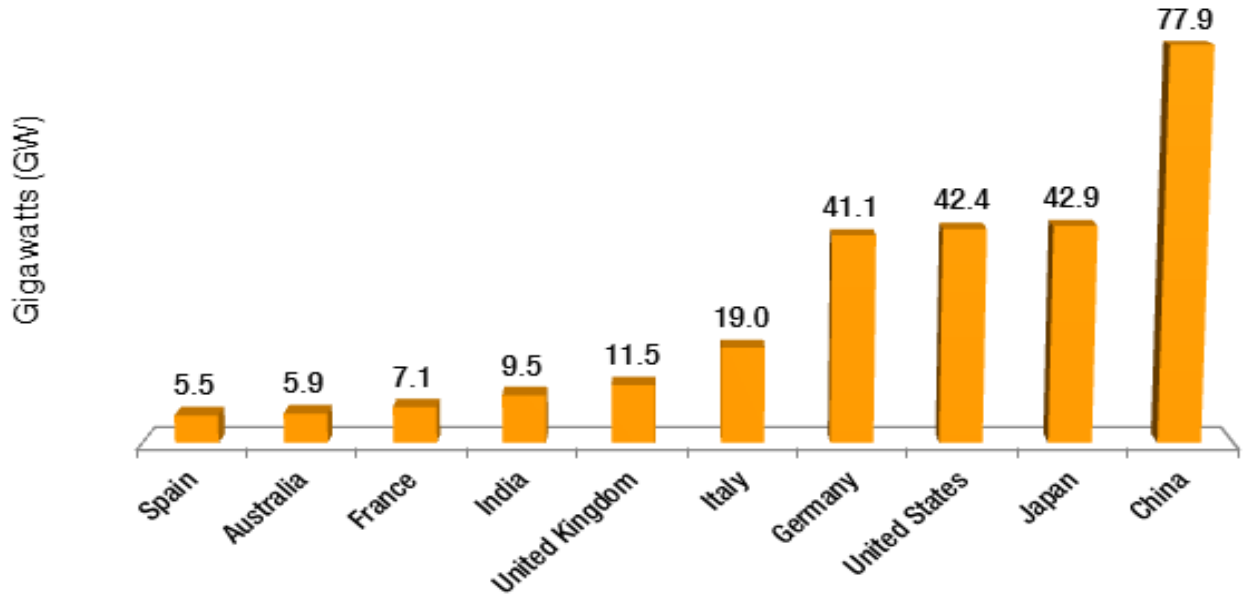

Figure 1.2.

1.3 Proposed Method

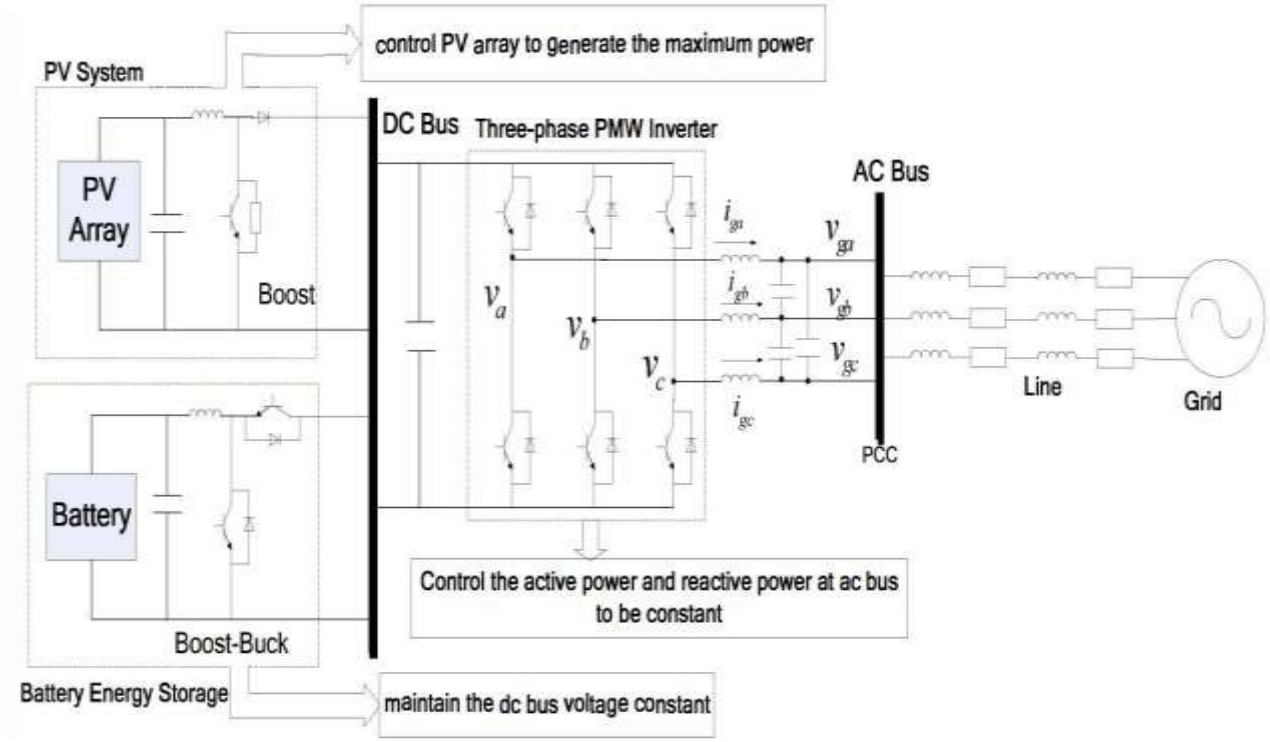

Figure 1.3. Configuration of the grid-connected PV /Battery generation system

PV array and battery are connected to the common dc bus via a **DC-DC converter** respectively, and then interconnected to the ac grid via a common DC/AC inverter. Battery

energy storage can charge and discharge to help balance the power between PV generation and loads demand. When the generation exceeds the demand, PV array will charge the battery to store the extra power, meanwhile, when the generation is less than the demand, the battery will discharge the stored power to supply loads. Each of PV system, battery energy storage system and the inverter has its independent control objective, and by controlling each part, the entire system is operating safely.

Here , Battery is incorporated with Bi-directional converter which works as BUCK & BOOST mode according to demand.

The output, we get from boost converter is DC. In order to synchronize this output with household use and local grid , DC-AC conversion is required. Three-phase VSI is needed with L filter in this purpose. Due to fluctuation of weather (Solar irradiance & temperature) , PI controller is used for componsetation.

1.4 PV Technology

Solar Cell Structure

A solar cell is an electronic device which directly converts sunlight into electricity. The mechanism in which solar light is directly converted into voltage or current is called the photovoltaic effect.

Basic steps in the operation of a solar cell are:

a. The generation of light generated carriers (electrons and holes): due to the absorption of incident photons by the material (semiconductor, typically silicon: Si) to create electron-hole pairs provided that the incident photon has an energy greater than that of the band gap.

b. **.** The collection of the light-generated carriers by the p-n junction to generate a current: due to the existing electric field at the p-n junction, the p-n junction spatially separates the electron (to the n-type zone) and the hole (to the p-type zone) to prevent its recombination. Modelling, Control and Simulation of a microgrid

c. The collection of the light-generated carriers by the p-n junction to generate a current: due to the existing electric field at the p-n junction, the p-n junction spatially separates

the electron (to the n-type zone) and the hole (to the p-type zone) to prevent its recombination. Modelling, Control and Simulation of a microgrid .

d. The collection of the charge carriers at the contacts and the generation of a large voltage across the solar cell.

e. The dissipation of power in the load and in parasitic resistances.

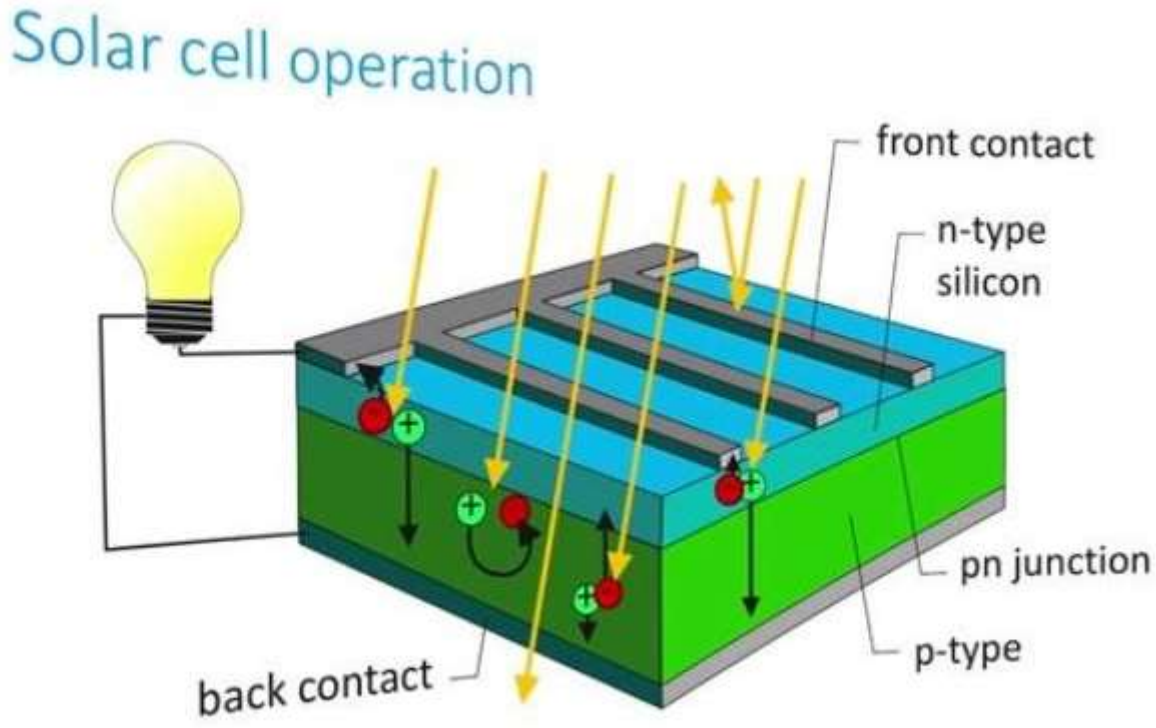

Figure 1.4. A representation scheme of the solar cell operation

1.5 PV Array Modelling

Photovoltaic cell is the most basic generation part in PV system. Single-diode mathematic model is applicable to simulate silicon photovoltaic cells, which consists of a photocurrent source I_{ph} a nonlinear diode, internal resistance es R_s and R_{sh} as shown in figure

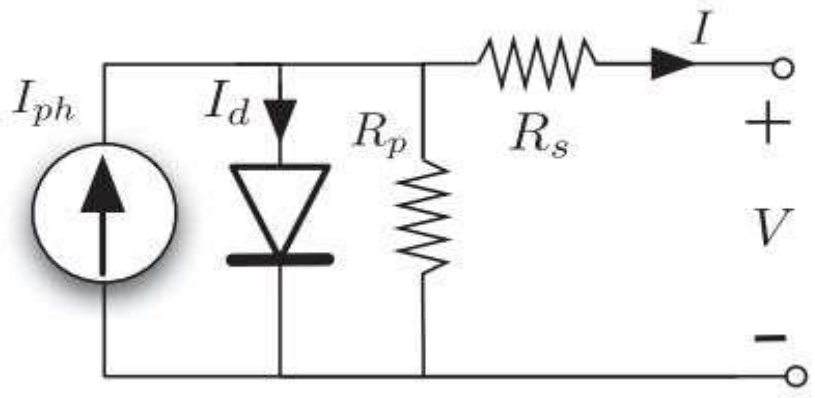

Figure 1.5.

Single-diode mathematic model of a PV cell

The mathematic relationship for the current and voltage in the single-diode equivalent circuit can be described as:

$$I = \boldsymbol{I_{ph}} - \boldsymbol{I_s}\left(e^{\frac{q(V+IR_S)}{AkT}} - 1\right) - \frac{V+IR_s}{R_{sh}} \qquad \ldots\ldots\ldots\ldots\ldots\ldots \textbf{(1)}$$

where, $\boldsymbol{I_{ph}}$ is photocurrent; I, is diode saturation current; q is coulomb constant (1.602e·19C) ; k is Boltzman's constant (1.381e-23 J/K) ; T is cell temperature (K) ; **A** is P-N junction ideality factor; $\boldsymbol{R_s}$ and $\boldsymbol{R_{sh}}$ are intrinsic series resistances.

Photocurrent is the function of solar radiation and cell temperature, described as :

$$\boldsymbol{I_{ph}} = \left(\frac{S}{S_{ref}}\right)\left[\boldsymbol{I_{ph,ref}} + \boldsymbol{C_T}\left(\boldsymbol{T} - \boldsymbol{T_{ref}}\right)\right] \quad \ldots\ldots\ldots\ldots\ldots \textbf{(2)}$$

where, S is the real solar radiation (W/m^2); $\boldsymbol{S_{ref}}, \boldsymbol{T_{ref}}, \boldsymbol{I_{ph,ref}}$ is the solar radiation, cell absolute temperature, photocurrent in standard test conditions respectively; C_T is the temperature co-efficient (A/K).

Diode saturation current varies with the cell temperature.

$$I_s = I_{s,ref}\left(\frac{T}{T_{ref}}\right)^3 e^{\left[\frac{qE_g}{Ak}\left(\frac{1}{T_{ref}}-\frac{1}{T}\right)\right]} \quad \ldots\ldots\ldots\ldots\ldots(3)$$

where. $I_{s,ref}$ is the diode saturation current in standard test conditions; **Eg** is the band-gap energy of the cell semiconductor (eV), depending on the cell material. When PV cells are arranged together in series and parallel to form arrays, these cells are usually considered to have the same characteristics. The equivalent circuit of PV array can be described as **figure [8]**.

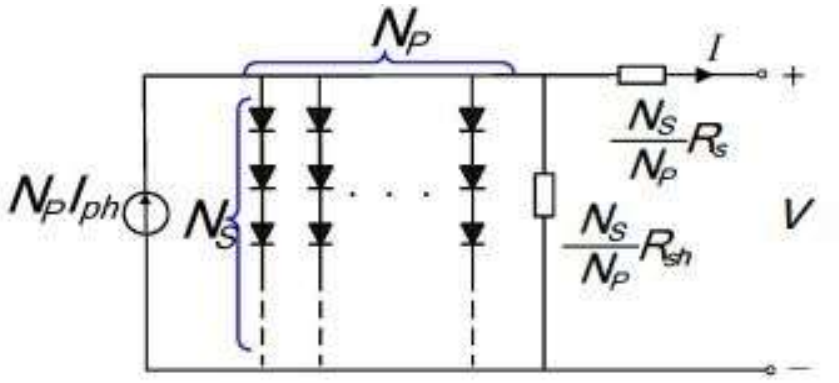

Figure 1.6

The relationship of the voltage and current in PV array is:

$$I = N_p I_{ph} - N_p I_s\left(e^{\frac{q}{AkT}\left(\frac{V}{N_S}+\frac{IR_S}{N_p}\right)} - 1\right) - \frac{N_p}{R_{sh}}\left(\frac{V}{N_s}+\frac{IR_s}{N_p}\right) \ldots\ldots..(4)$$

where, N_s and N_p are cell numbers of the series and parallel cells respectively.

PARAMETERS FOR PV MODEL

Parameters	Values
Referenced solar irradiance S_{ref}	$1000 W/m^2$
Referenced cell temperature T_{ref}	$298\ K$
Cell numbers of a PV module m	36
Parallel numbers of the PV modules N_P	9
Series numbers of the PV modules N_S	20
Photocurrent at standard condition $I_{ph,ref}$	$3.35\ A$
Band-gap energy $E_g\ (eV)$	$1.237\ eV$
Cell internal resistance R_s	$0.312\ \Omega$
P-N junction ideality factor A	54
Temperature coefficient C_T	0.065%

1.6 MATLAB Code of PV Characteristics Curve

```
clc;
clear all;
q=1.6e-19; Tr=25+273;
Iscr=8.449; Voc=37.191;
Ns=60; Np=1; A=1.3; k=1.38e-23;
Rs=0.05; Rp=100;
S=1200;
Eg=1.12;
T=25+273;
Vt=Ns*k*T/q;
Ki=0.0;
Ipv0=2;

Iph=(Iscr+Ki*(T-Tr))*S/1000;
Irs=Iscr/(exp(q*Voc/(Ns*k*Tr))-1);
Is=Irs*(T/Tr)^3*exp(q*Eg/(A*k)*(1/Tr-1/T));
```

```
Vpv=0:0.1:37;
for i=1:length(Vpv)
Ipv(i)=fsolve(@(Ipv) -Ipv+Iph-Is*exp((Vpv(i)+Ipv*Rs)/Vt)-
(Vpv(i)+Ipv*Rs)/Rp, Ipv0,
optimoptions('fsolve','Display','off'));
end

subplot(1,2,1)
plot(Vpv,Ipv)
subplot(1,2,2)
plot(Vpv,Vpv.*Ipv)
```

1.7 Simulation Results

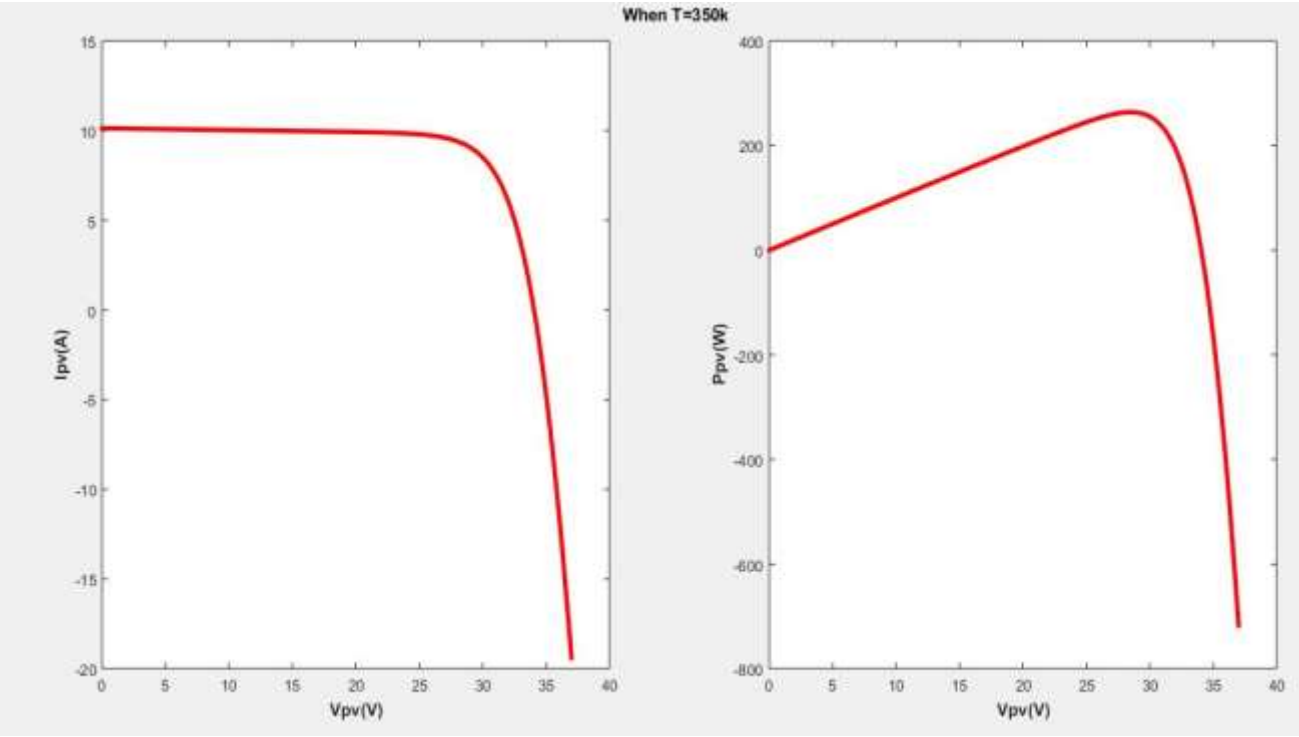

Figure 1.7

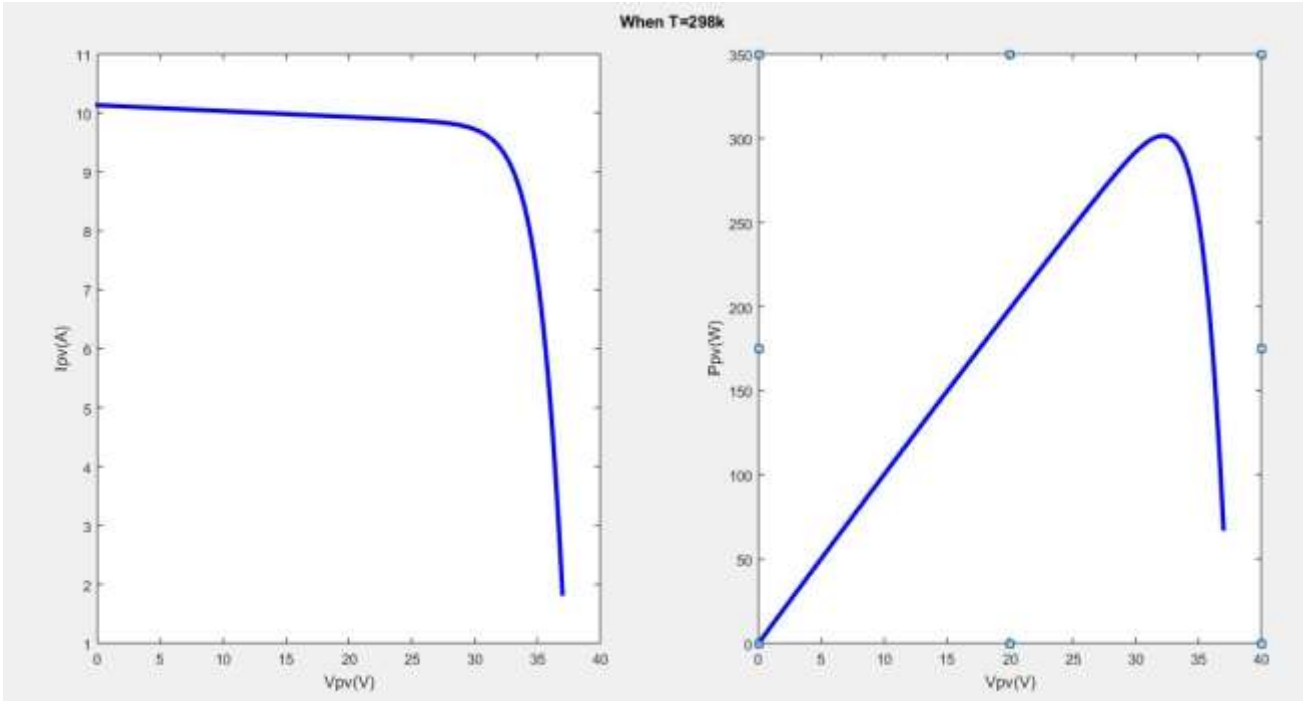

Figure 1.8.

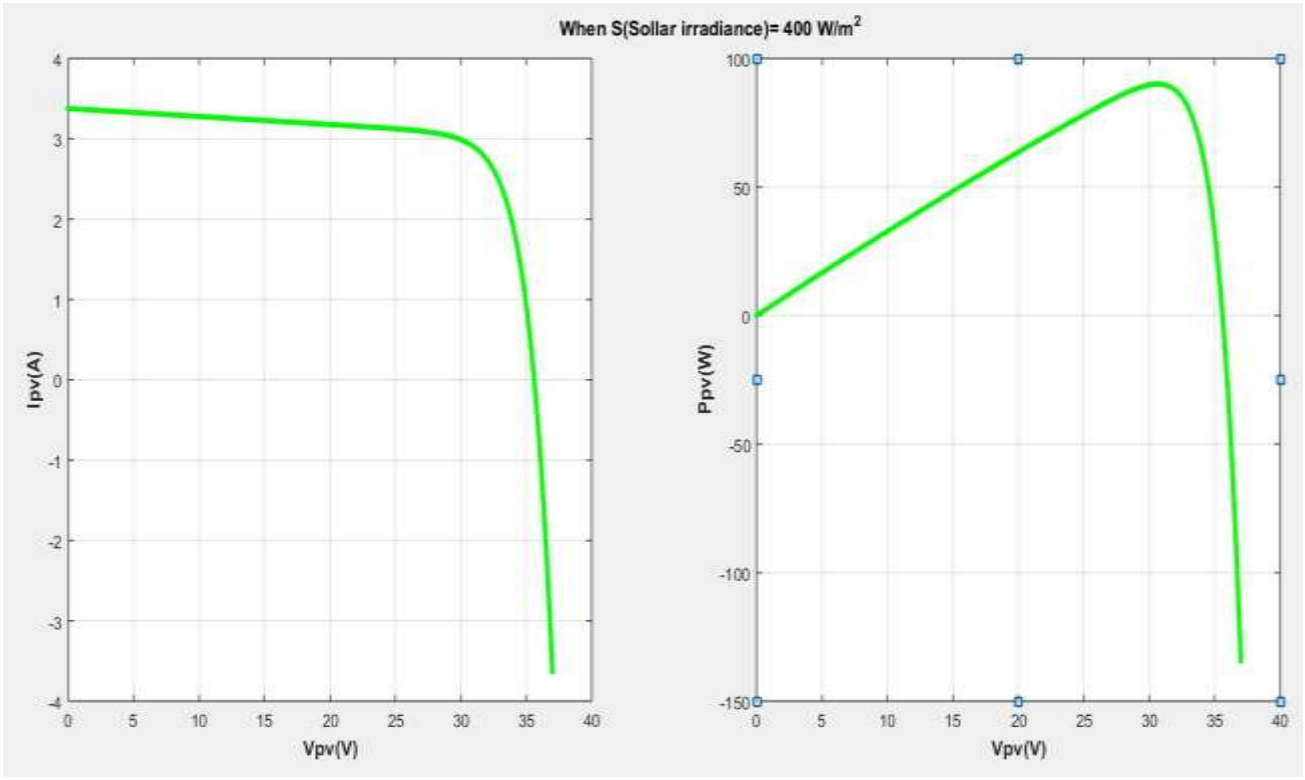

Figure 1.9.

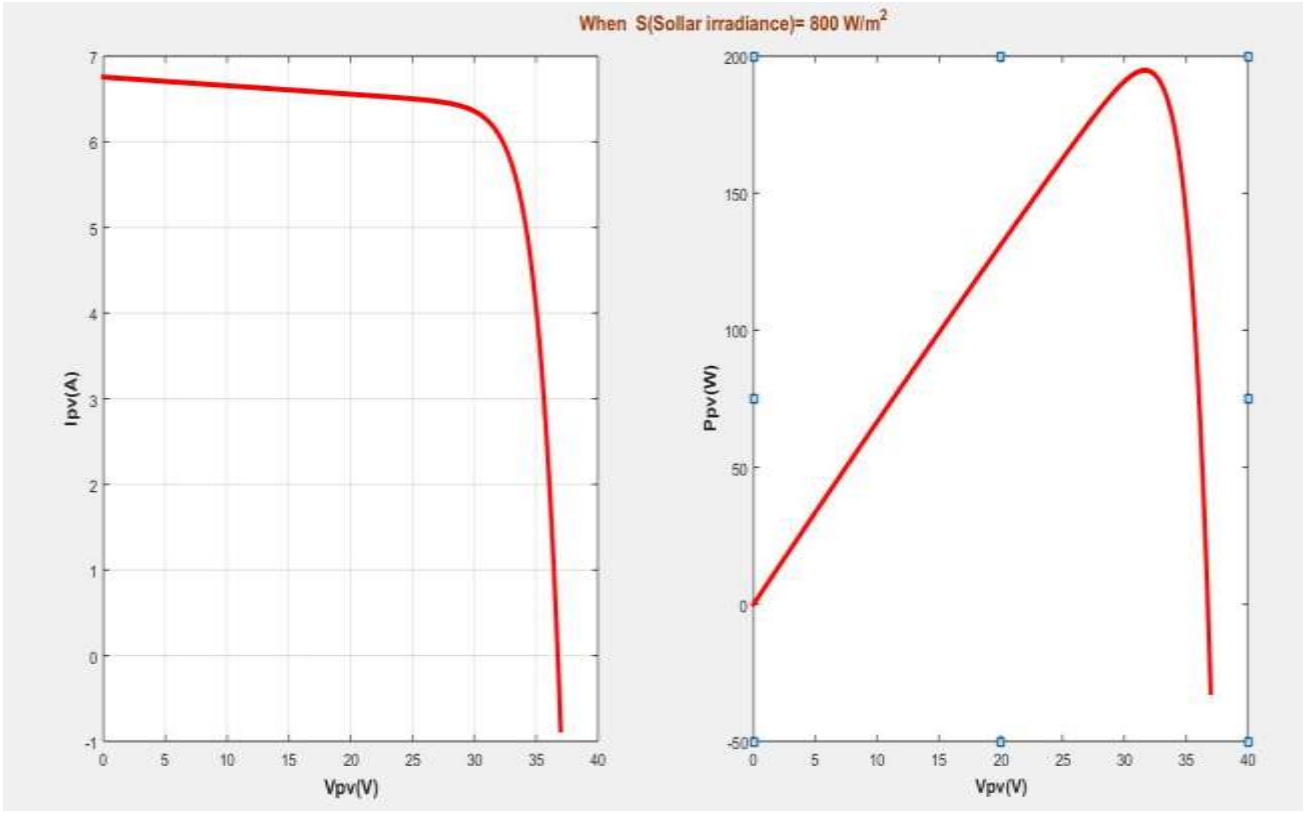

Figure 1.10

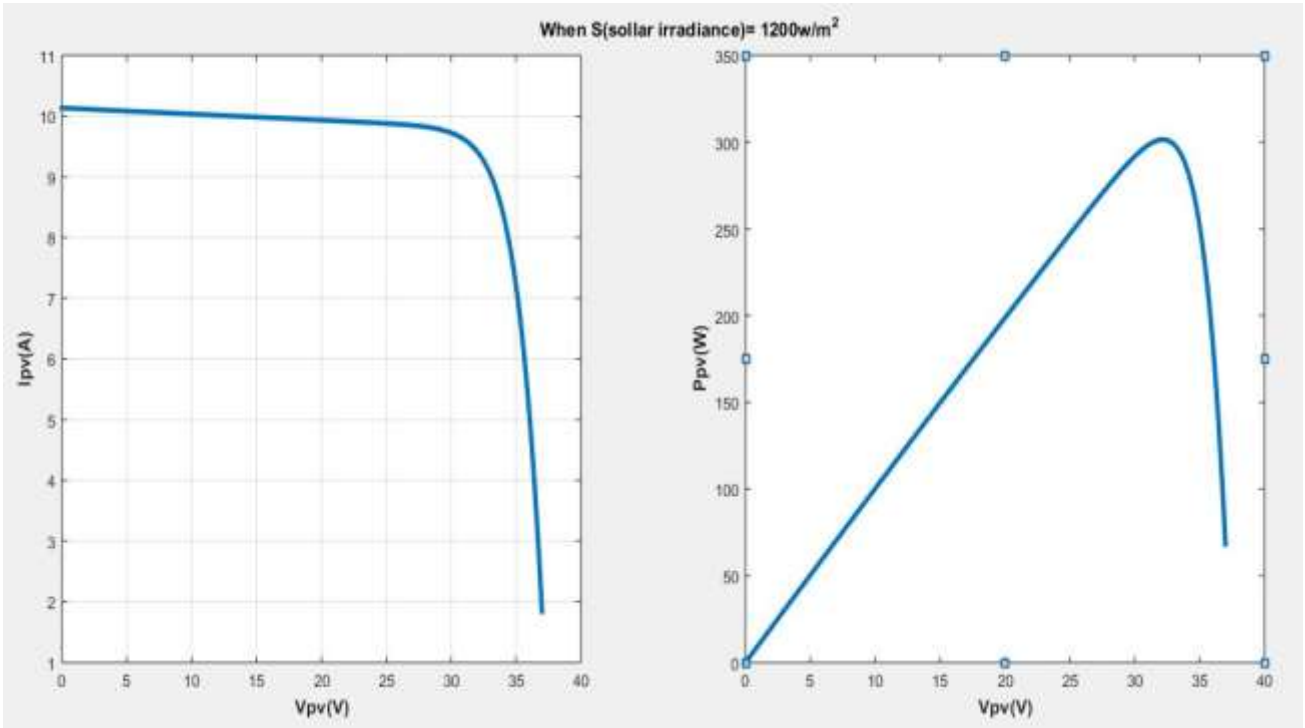

Figure 1.11.

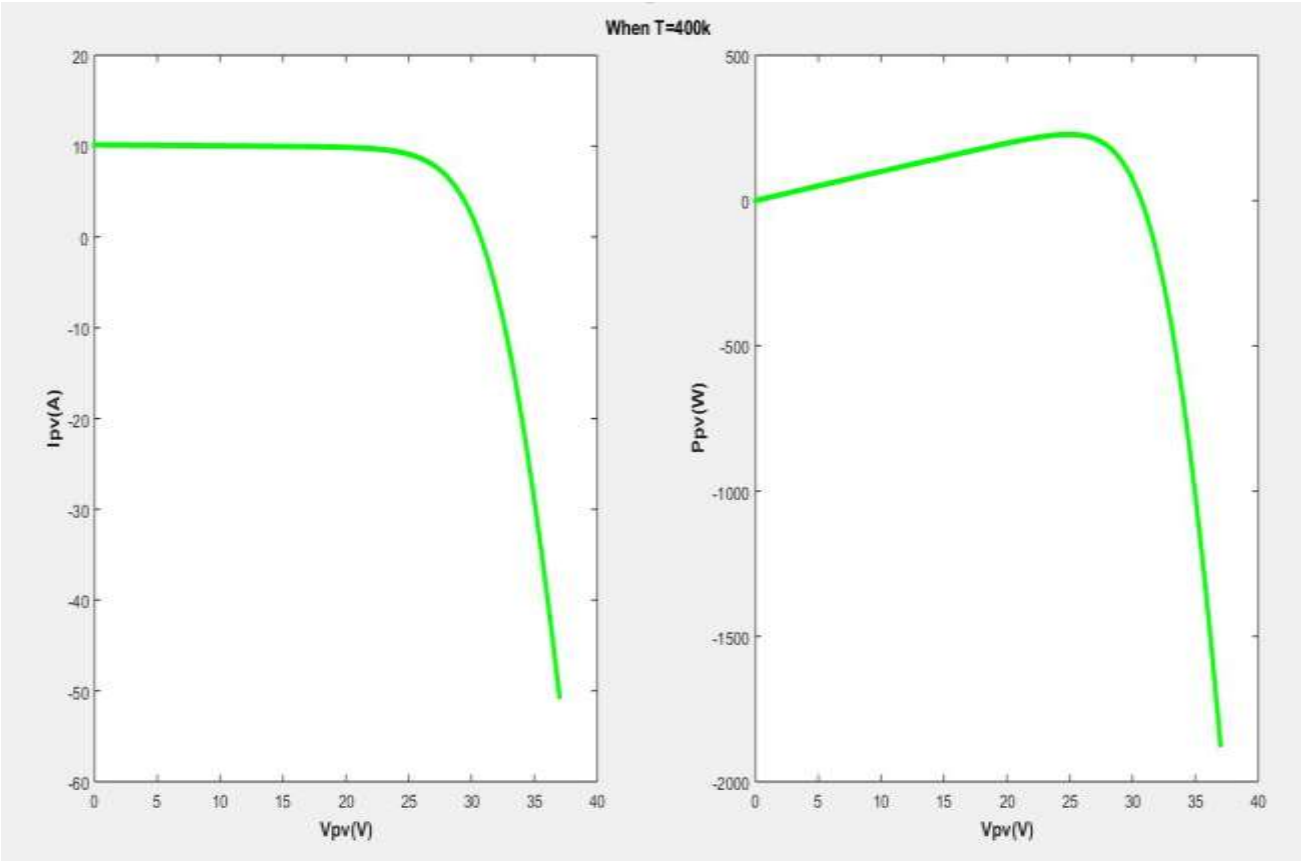

Figure 1.12

CHAPTER 2

DC-DC Converter

2.1. Classification

A **DC-DC Converter** is an electronic circuit or electromechanical device that converts a source of direct current (DC) from one voltage level to another. It is a type of electric power converter. Power levels range from very low (small batteries) to very high (high-voltage power transmission).

With the voltage and current relationship, influencing factors for the equilibrium of the converter such as the capacitor's voltage ripple and inductor voltage-second balance condition have been derived. Similar analysis can also be done for the other types of converters. Basic circuit diagram of all the fundamental converters are shown in Figure 1. They consist of the same basic elements. The building blocks of these converters are DC supply Vs, load, diode D, power electronics switch S, inductor L, and capacitor C.

Types of DC-DC converter :

i. Buck Converter or Step-down converter

ii. Boost Converter or Step-up Converter

iii. Buck-Boost Converter

iv. Cuk Converter

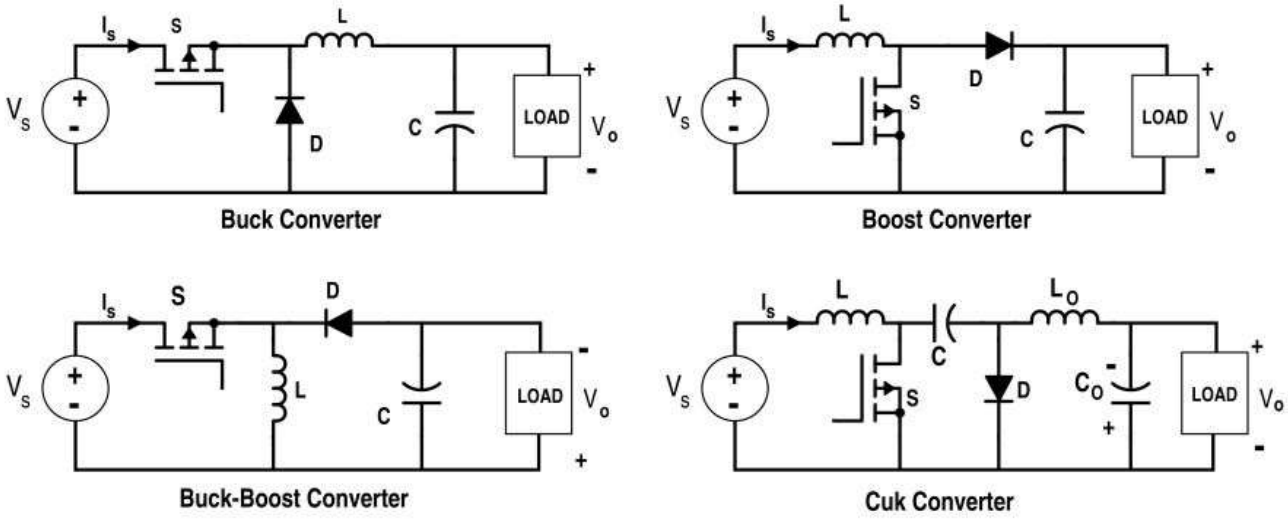

Figure 2.1. Different types of DC-DC Converter

It is worth noticing that any converters work in two distinct modes with respect to the inductor current: the continuous conduction mode (CCM) and discontinuous conduction mode (DCM). When the inductor current is always greater than zero, it is in CCM. When the average inductor current is too low due to the high-load resistance or low-switching frequency, then the converter is in DCM. The CCM is preferable for high efficiency and efficient use of semiconductor switches and passive components. The DCM requires a special control since the dynamic order of the converter is reduced. Thus, it is required to find out the minimum value of the inductor to maintain the CCM.

Assume that the inductor and capacitor are pure (i.e. no resistive component). However, there is still what we call a small-ripple approximation. In an efficient converter, the output voltage ripple is small.

It is assumed that the load is resistive and the DC component of the output voltage has no ripples, or simply the DC output has a fixed value as shown in Fig.2 for making the analysis easier. So,

$\Delta V_o = 0$ and $V_o = V_{dc}$

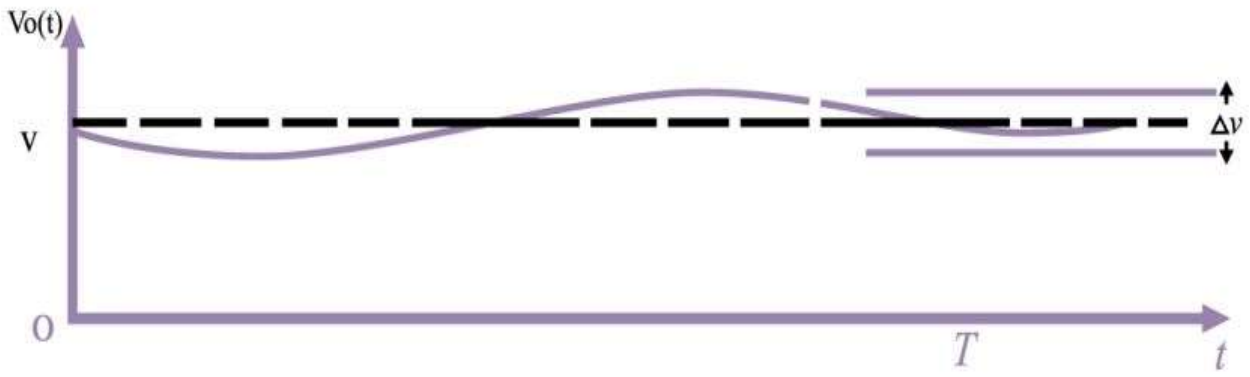

Figure 2.2.

Under certain duty cycles, voltage production is medium in Cuk converter, lower in Buck and Buck-Boost converter and higher in Boost converter [19].

Besides, the voltage we need to have at the end of a DC-DC converter has to be more higher than the initial voltage we get from solar PV panel to provide sufficient DC voltage to the bus so that the inverter can render higher value AC voltage to the grid.

These are the reason we choose Boost converter over other DC-DC converters.

2.2 State-space averaging technique

This technique derives the generalized equation for the continuous mode of the basic power converters. The continuous mode operation is simpler as there are only two states. The analysis

starts from the state-space equations during the transistor's on and off states and uses an averaging method to linearize them. When the switching device is turned on, it conducts for a ratio D of a period. The state space equation can be written as:

$$\dot{X} = A_{on} X + B_{on} Y \ldots\ldots\ldots\ldots\ldots\ldots\ldots\ldots\ldots(1)$$

When the switching device is turned off, the diode conducts for a ratio of (1-D) of a period. The state space equation can be written as:

$$\dot{X} = A_{off} X + B_{off} Y \ldots\ldots\ldots\ldots\ldots\ldots\ldots\ldots (2)$$

where X is the state space variable such as capacitor voltage and inductor current, i.e.$[i_L\ v_c]^T$. A_{on}, B_{on} and A_{off} and B_{off} are the state-space matrices of the converter during the on- and off-states respectively. Y is the input variable such as input voltage V_{in} .

Because on- and off-states are presented for D and 1-D duration, they can be averaged by the conduction ratio[5]:

$$\dot{X} = [\ DA_{on} + (1\text{-}D)A_{off}\ ]\ X + [\ DB_{on} + (1\text{-}D)B_{off}\ ]\ Y \ldots\ldots\ldots\ldots(3)$$

Now, consider there is a small signal variation d to the duty ratio D that will cause a small variation x of the state variable X. Therefore assume the variation of the small signal can be written as:

$$D = \overline{D} + d \ldots\ldots\ldots\ldots\ldots\ldots\ldots\ldots\ldots\ldots(4)$$

$$X = \overline{X} + x \ldots\ldots\ldots\ldots\ldots\ldots\ldots\ldots\ldots\ldots (5)$$

i.e. x is a small-signal variation in the DC or steady-state component $\bar{X}$ and d is a small signal variation in the steady-state or DC component duty-ratio $\overline{D}$. Equation (3) becomes:

$$\dot{\overline{X}} + \dot{x} = [(\overline{D} + d)A_{on} + (1 - \overline{D} - d)A_{off}\ ]$$

$$+[\overline{X}+x]+[(\overline{D}+d)B_{on}+(1-\overline{D}-d)B_{off}\,]Y \ \ldots\ldots\ldots(6)$$

which can be expanded to:

$$\dot{\overline{X}}+\dot{x} = [(\overline{D}A_{on}+(1-\overline{D})A_{off}\,]\overline{X}+[\overline{D}B_{on}+(1-\overline{D})B_{off}\,]Y$$

$$+[\,d\,A_{on}-d\,A_{off}\,]\overline{X}+[\,d\,B_{on}-d\,B_{off}\,]Y$$

$$+[(\overline{D}A_{on}+(1-\overline{D})A_{off}\,]x+[\,d\,B_{on}-d\,B_{off}\,]x \ \ldots\ldots\ldots\ldots\ldots(7)$$

Equation (3) can be re-written as follows if the small signal is zero:

$$\dot{\overline{X}} = [(\overline{D}A_{on}+(1-\overline{D})A_{off}\,]X+[\overline{D}B_{on}+(1-\overline{D})B_{off}\,]Y\ldots\ldots\ldots\ldots\ldots\ldots\ (8)$$

Eliminate equation (8) from (7) and neglect the high order small signal variation, and it follows that

$$\dot{x} = Ax + Fd \ \ldots\ldots\ldots\ldots\ldots\ldots\ldots\ldots\ldots\ (9)$$

where $A = \overline{D}A_{on} + (1-\overline{D})\,A_{off}$ .....(10)

and $F = [\,A_{on} - A_{off}\,]\,X + [\,B_{on} - B_{off}\,]Y \ \ldots\ldots\ldots\ldots\ldots(11)$

A is the average of A_{on} and A_{off} and F is the difference of equations (1) and (2) which is the difference between the on-state and off-state of X. Equation (9) is now a linearized equation and the original digital feature is removed. The equation can be easily be solved by conventional Laplace Transform.

$$\frac{x}{d} = [sI - A]^{-1} F \ldots\ldots\ldots\ldots\ldots\ldots\ldots\ldots\ldots\ldots \quad (12)$$

where I the unit matrix. $[\mathrm{sI} - \mathrm{A}]^{-1}$ is the inverse of $[\mathrm{sI} - \mathrm{A}]$. The next few sections apply the above equations to obtain the small signal response of the boost converter [20].

2.3 Small signal modelling of Boost Converter

A Boost converter is a popular circuit especially for power factor correction. The understanding of its frequency response is therefore important. The parameters for the energy storage element, i_L and v_C, again are used for the state-space variable. Similar methods based on transistor's on- and off-states are used. Fig. 1 shows the Boost converter [21].

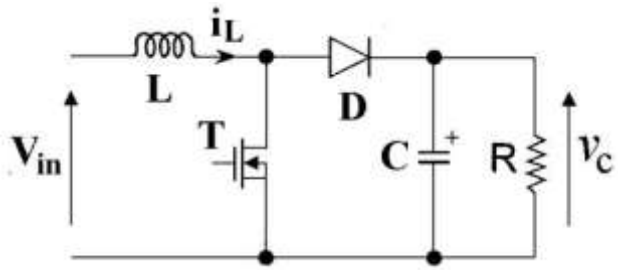

Figure 2.3. Boost Converter Circuit Diagram

Two modes of Boost converters are [22]

I. Mode 1: When switch is closed and diode is reverse biased

II. Mode 2: When switch is open and diode is forward biased

The following table describes the analysis of these modes.

Table 1. Equations for different modes of Boost Converter [22]

Mode 1	Mode 2
$\frac{dI_{pv}}{dt} = \frac{V_{pv}}{L}$	$\frac{dI_{pv}}{dt} = \frac{\left(V_{pv} - V_{dc}\right)}{L}$
$\frac{dV_{dc}}{dt} = -\frac{V_{dc}}{R_{dc}C}$	$\frac{dV_{dc}}{dt} = \frac{I_{pv}}{C} - \frac{V_{dc}}{R_{dc}C}$

2.3.1 Mode 1 Circuit Calculations

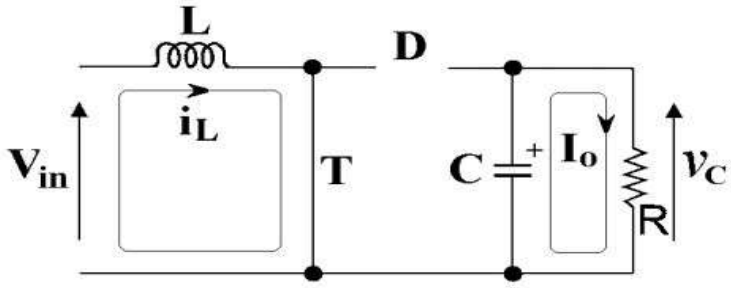

Figure 2.4. Equivalent Circuit for Mode 1

KVL at loop 1,

$-V_{pv} + V_L = 0 \quad \left[V_{pv} = V_{in}\right]$

$\rightarrow V_L = V_{pv}$

$\therefore \frac{dI_{pv}}{dt} = \frac{V_{pv}}{L}$

KVL at loop 2,

$V_{dc} + V_c = 0$

$\rightarrow V_{dc} = -V_c \quad [\because |V_{dc}| = |V_c|]$

$\rightarrow R_{dc}C\frac{dV_{dc}}{dt} = -V_c$

$\rightarrow \frac{dV_{dc}}{dt} = -\frac{V_c}{R_{dc}C}$

$$\therefore \frac{dV_{dc}}{dt} = -\frac{V_{dc}}{R_{dc}C}$$

Steady state equation for Mode1[21] is given by Equ. (1)

$$\dot{X} = [A_1][X] + [B_1][U]$$

State space matrix for Mode 1of Boost Converter[3]

$$\begin{bmatrix} \frac{dI_{pv}}{dt} \\ \frac{dV_{dc}}{dt} \end{bmatrix} = \begin{bmatrix} \dot{I_{pv}} \\ \dot{V_{dc}} \end{bmatrix} = \begin{bmatrix} 0 & 0 \\ 0 & -\frac{1}{R_{dc}C} \end{bmatrix} \begin{bmatrix} I_{pv} \\ V_{dc} \end{bmatrix} + \begin{bmatrix} \frac{1}{L} \\ 0 \end{bmatrix} [V_{pv}]$$

2.3.2 Mode 2 Circuit Calculations

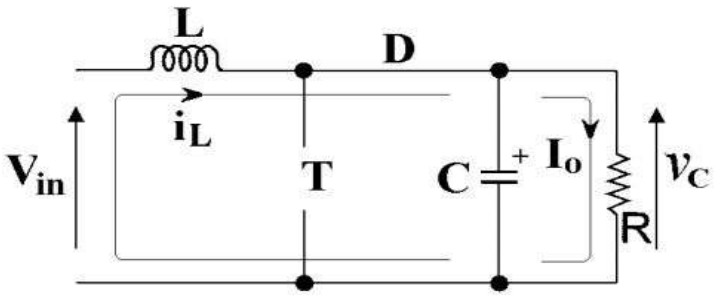

Figure 2.5. Equivalent Circuit for Mode 2

KVL at loop,

$$-V_{pv} + V_L + V_{dc} = 0 \qquad [V_{pv} = V_{in}]$$

$$\rightarrow V_L = -V_{dc} + V_{pv}$$

$$\rightarrow L\frac{dI_{pv}}{dt} = -V_{dc} + V_{pv} \qquad [V_{dc} = V_c]$$

$$\therefore \frac{dI_{pv}}{dt} = -\frac{V_{dc}}{L} + \frac{V_{pv}}{L}$$

KCL at node n,

$$I_{pv} = I_c + I_{R_{dc}}$$

$$\rightarrow I_c = I_{pv} - I_{R_{dc}}$$

$$\therefore \frac{dV_{dc}}{dt} = \frac{I_{pv}}{C} - \frac{V_{dc}}{R_{dc}C}$$

Steady state equation for Mode 2 is given by Equ. (2)

$$\dot{X} = [A_2][X] + [B_2][U]$$

State space matrix for Mode 2 of Boost Converter [19]

$$\begin{bmatrix} \dot{I_{pv}} \\ \dot{V_{dc}} \end{bmatrix} = \begin{bmatrix} 0 & -\frac{1}{L} \\ \frac{1}{C} & -\frac{1}{R_{dc}C} \end{bmatrix} \begin{bmatrix} I_{pv} \\ V_{dc} \end{bmatrix} + \begin{bmatrix} \frac{1}{L} \\ 0 \end{bmatrix} [V_{pv}]$$

2.3.3 Forming overall state Space Matrix

Matrices [A] and [B] are obtained by using (3) and (4) respectively using state space averaging technique

$$A = A_1 D + A_2(1 - D) \qquad (3)$$

$$[A] = \begin{bmatrix} 0 & 0 \\ 0 & -\frac{1}{R_{dc}C} \end{bmatrix} D + \begin{bmatrix} 0 & -\frac{1}{L} \\ \frac{1}{C} & -\frac{1}{R_{dc}C} \end{bmatrix} (1 - D)$$

$$\therefore [A] = \begin{bmatrix} 0 & -\frac{(1-D)}{L} \\ \frac{(1-D)}{C} & -\frac{1}{R_{dc}C} \end{bmatrix}$$

$$B = B_1 D + B_2(1 - D) \qquad (4)$$

$$[B] = \begin{bmatrix} \frac{1}{L} \\ 0 \end{bmatrix} D + \begin{bmatrix} \frac{1}{L} \\ 0 \end{bmatrix} (1 - D)$$

$$\therefore [B] = \begin{bmatrix} \frac{1}{L} \\ 0 \end{bmatrix}$$

Steady state equation for boost converter is given by

$$\dot{X} = [A][X] + [B][U]$$

State space matrix for Boost Converter

$$\begin{bmatrix} \dot{I_{pv}} \\ \dot{V_{dc}} \end{bmatrix} = \begin{bmatrix} 0 & -\frac{(1-D)}{L} \\ \frac{(1-D)}{C} & -\frac{1}{R_{dc}C} \end{bmatrix} \begin{bmatrix} I_{pv} \\ V_{dc} \end{bmatrix} + \begin{bmatrix} \frac{1}{L} \\ 0 \end{bmatrix} \begin{bmatrix} V_{pv} \end{bmatrix}$$

Chapter 3

Battery Energy Storage System Integrated With Bidirectional Converter For Grid Connected PV

3.1. Grid Scale Energy Storage

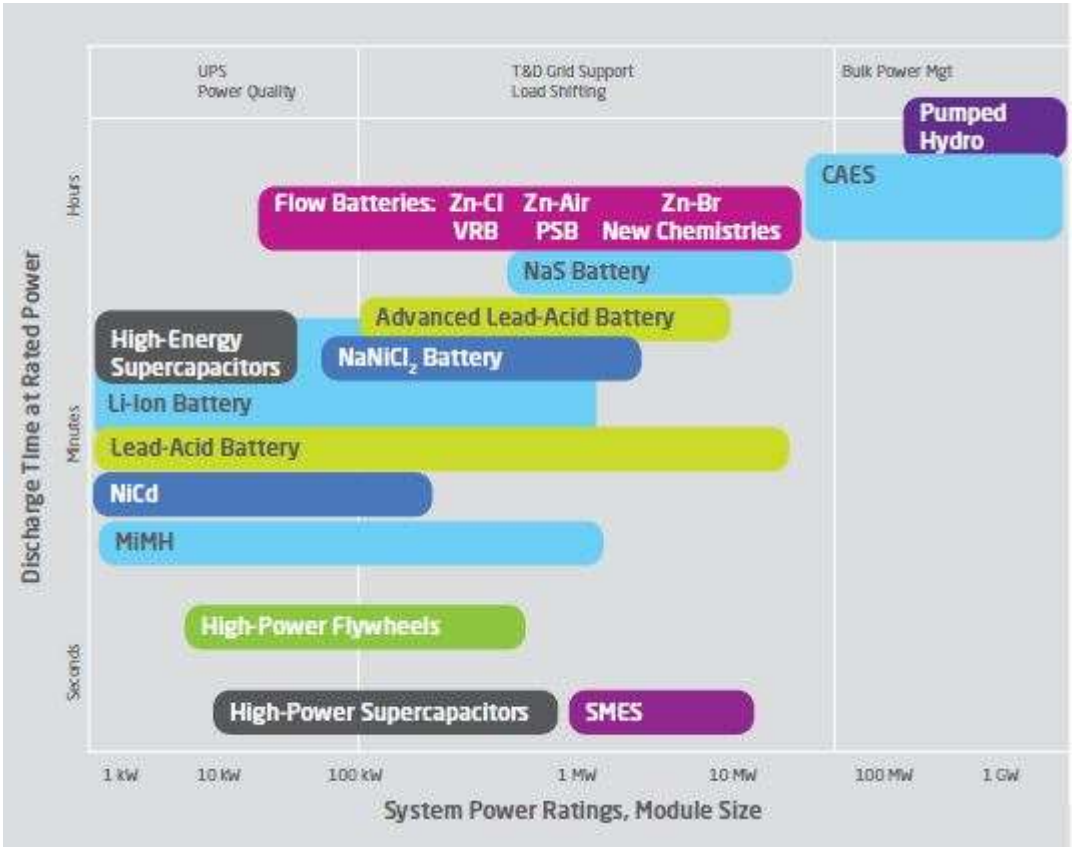

Figure 3.1

3.2 Application Of BESS For Grid Integration

Battery storage in the power sector can be employedin a variety of ways over multiple time periods, ranging

from seconds to hours. EPRI and DOE (2013) describe14 services under five umbrella groups that can generallybe provided by energy storage. These include bulkenergy, ancillary services, transmission infrastructure,distribution infrastructure and customer managementservices. Battery storage can, in principle, provide allthese services. Figure 6 below outlines the categoriesand subcategories of these services. This report focuseson those highlighted in red through the applicationareas presented below. The application areas discussed here were determined by examining the applications of battery storage most directly related to wind and solar PV power integration. The emphasis was on those that have been demonstrated and/or deployed in the market. These applications compensate for the variable nature of wind and solar power. They match supply of renewable resources with demand, and optimise variable renewable energy feedin to the grid. They also provide or take away power when supply and demand become out of balance. It is important to note that a single battery installation can serve multiple uses. A combination of value

streams may benefit the economics of an installation. In the following section, the use of battery storage is discussed for the several applications. These are islands and off-grid scenarios (which can encompass all the services highlighted in red in figure 6), and households with solar PV (power reliability and retail electric energy time shift). Additionally, variable renewable energy smoothing and supply shift (electric energy time shift are discussed). Finally, regulation (ancillary services) in grids with high variable renewable energy shares is explored, with emphasis on short-term regulation at the grid level.

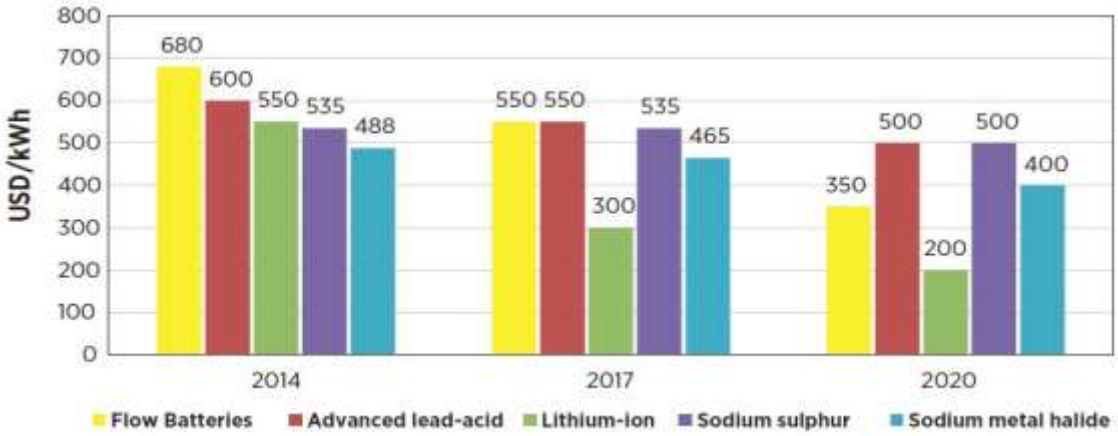

Figure 3.2

3.3. Electrical Equivalent Circuit Model Of Battery

In this experiment, zeroeth order, first order, and second order Randle equivalent circuit models were considered. Each of these models had advantages and disadvantages that needed to be considered. The lower the model order, the less parameters that needed to be identified. However, as model order decreased, the model‟s voltage response became less and less representative of a real battery. These characteristics need to be balanced, and here the pros and cons of the three orders of models that were considered are described in detail.

3.3.1 Zeroth Order

The zeroeth order equivalent circuit model was the simplest model and consisted of only two elements, an ideal voltage source and a resistor as seen in Figure 9. The resistor in this model represented the internal resistance of the battery, R_0, and the voltage source represented the open circuit voltage E_0. Although equivalent circuit models appear trivial, they are actually much more complicated due to the complexity of the parameters they contain. This simple model contained only two parameters to identify, however, the parameters in equivalent circuit models are not constant values. In this case, E_0 and R_0 are both functions are SoC, temperature, current direction (charge or discharge), and age. We can simplify these parameters in this project because all experiments occurred at constant temperature. Further simplifications were made for E_0 and R_0 as well. Open circuit voltage was assumed to depend only on SoC, and only current direction was considered for internal resistance because the small depth of discharge seen in this experiment was not believed to contribute significant variations in resistance due to state of charge.

Although this model was simple to identify, it would have provided an extremely poor representation of actual battery voltage response. From equation 1 we can see this model failed to capture the dynamics that are present in battery response. The response of this zeroeth order model would appear as a square wave pattern centered around E_0, with amplitude equal to IR_0. For these reasons, the zeroeth order model was not chosen to simulate battery behavior.

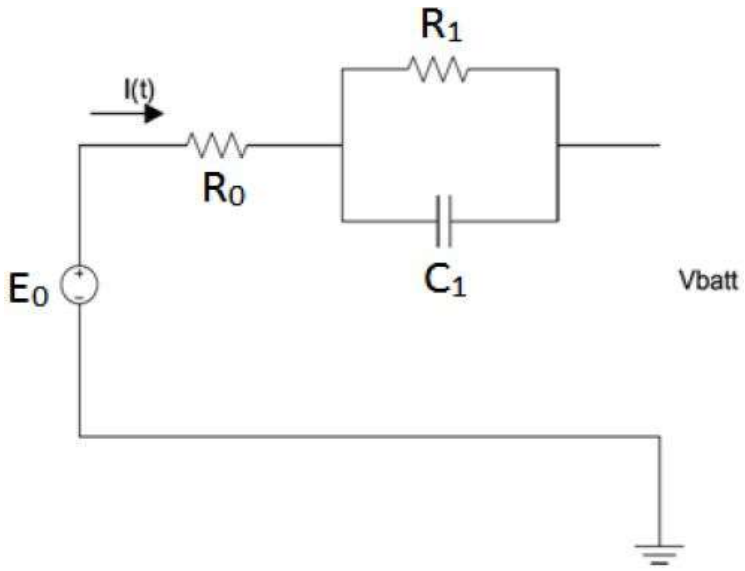

Figure 3.3: An example of different subcarrier mapping schemes for N = 4, Q = 3 and M = 12.

$$V = E_0 - R_0 I - V_{C1}$$

$$\frac{dV_{C1}}{dt} + \frac{1}{R_1 C_1} V_{C1} = \frac{1}{C_1}$$

$$E_0 = f(SoC, T)$$

$$R_0, R_1, C_1 = f(SoC, T, \text{sign}(I))$$

$$\alpha_1 = \frac{1}{R_1 C_1}$$

3.3.2 First Order

The first order battery model was a much closer approximation than the zeroeth order model to true battery voltage response. As we can see from Figure 10, the first order model contained one resistor /

capacitor pair in addition to the elements contained in the zeroeth order model. This resistor capacitor pair added two extra parameters to the system, a resistance and a capacitance, and resulted in a much better representation of true battery voltage response. The added resistance and capacitance were both dependent on current direction, SoC, and temperature, but the same assumptions made for internal resistance before were applied to both parameters.

The added resistor /capacitor pair was responsible for adding first order dynamics to the system, described by equations 4 and 5. This first order system was a much closer approximation of true battery behavior, but required more computational power than a simple zeroeth order model. Instead of identifying 3 parameters as in a zeroeth order system (E_0,R_{0c}, and R_{0d}), we are now required to identify seven; E_0, R_{0c}, R_{0d}, R_{1c}, R_{1d}, C_{1c}, C_{1d}, where c and d represent charge and discharge respectively..

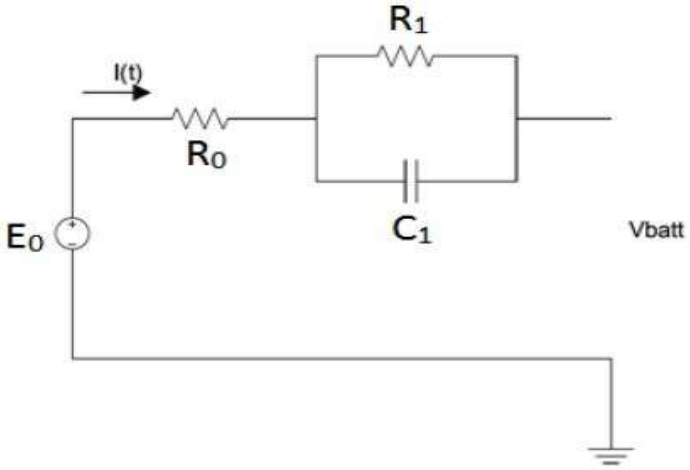

Figure 3.3.

$$V = E_0 - R_0 I - V_{C1}$$

$$\frac{dV_{C1}}{dt} + \frac{1}{R_1 C_1} V_{C1} = \frac{1}{C_1}$$

$$E_0 = f(SoC, T)$$

$$R_0, R_1, C_1 = f(SoC, T, \text{sign}(I))$$

$$\alpha_1 = \frac{1}{R_1 C_1}$$

3.3.3 Second Order

The second order model was very similar to the first order in appearance, the only difference was an additional resistor / capacitor pair as seen in Figure 11. These additional components added four extra parameters to the battery model, a charge and discharge value for the second resistor and capacitor, bringing the total number of parameters that needed to be identified up to eleven. At this point, model identification required significant computing time and power, making this model of little use in a real time application like that of vehicle diagnostics. However, these added parameters did increase the accuracy of the second order model, as seen in Figure 12. The addition of the second resistor capacitor pair stacked a second, first order dynamic system, on top of the one obtained in the first order model. To clarify, the second order model did not introduce second order dynamics, it merely summed the effects of two sets of first order dynamics as seen in equations 9, 10, and 11, allowing the model to represent a wider range of battery responses. It was because of this increased versatility that a second order model was chosen for use in simulating battery voltage and identifying battery parameters.

$$V = E_0 - R_0 I - V_{C1} - V_{C2}$$

$$\frac{dV_{C1}}{dt} + \frac{1}{R_1 C_1} V_{C1} = \frac{1}{C_1}$$

$$\frac{dV_{C2}}{dt} + \frac{1}{R_2 C_2} V_{C2} = \frac{1}{C_2}$$

$$E_0 = f(SoC, T)$$

$$R_0, R_1, R_2, C_1, C_2 = f(SoC, T, \text{sign}(I))$$

$$\alpha_1 = \frac{1}{R_1 C_1}$$

$$\alpha_2 = \frac{1}{R_2 C_2}$$

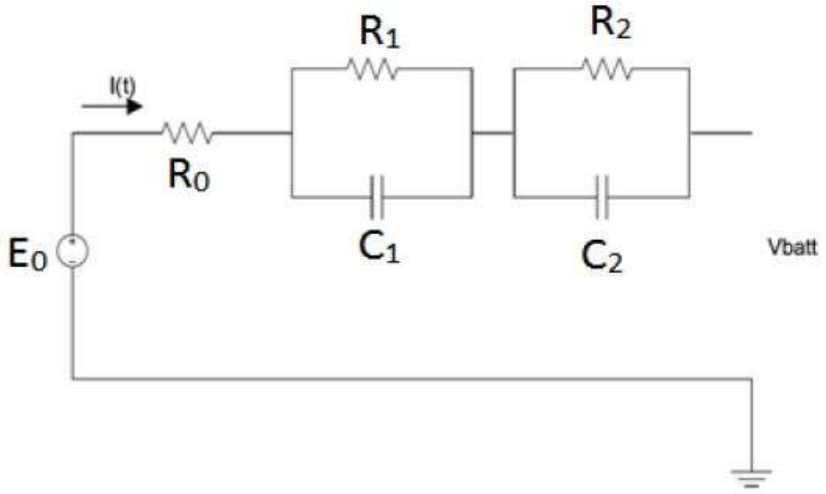

Figure 3.4.

3.4 System Architecture Of BESS+BDC

In this project, the PV+BESS system includes four major parts: AC grid side and AC load, AC/DC active rectifier, DC/DC converter, and PV generation and batteries. AC/DC rectifier is connected through L_{ac} which represents the combined inductance of the transformer and line on the grid side. The DC/DC converter is directly connected to the battery. The AC/DC rectifier is connected to the DC/DC converter through a DC-link capacitor C_{dc}. It is assumed that the grid side resistance and the loss of the DC link are negligible. The DC-link capacitor also works as part of the bidirectional DC/DC converter which can charge and discharge the battery. Detailed explanation will be presented in the coming sections.

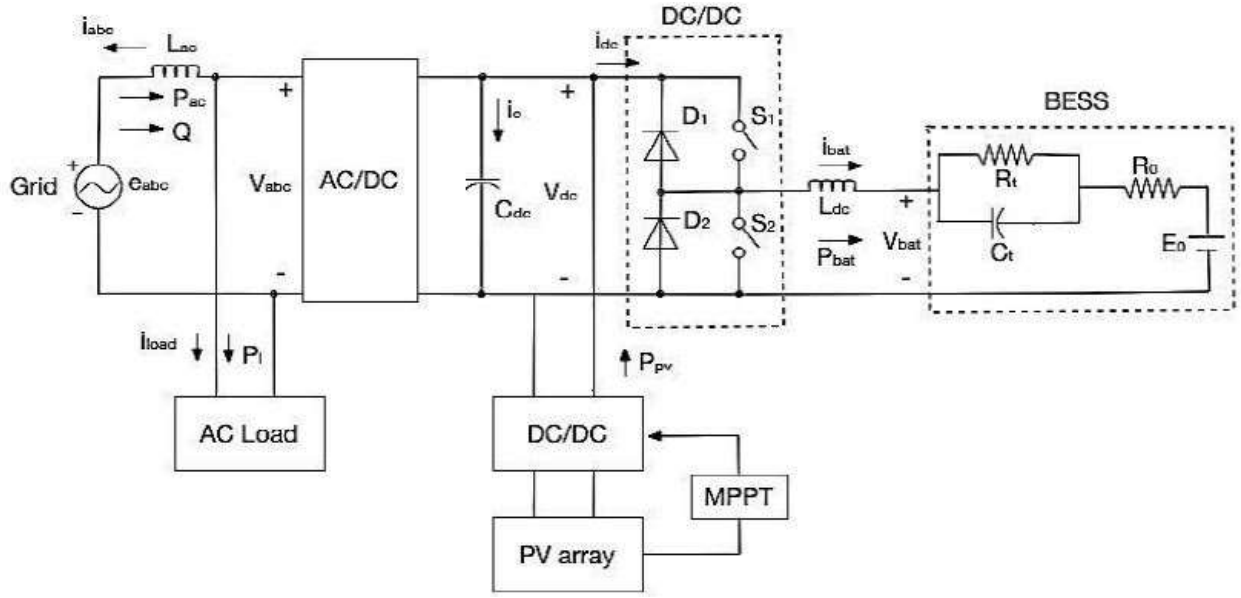

Figure 3.5: System Schematic Diagram.

3.5 Power Management

For the system above, several operation modes can be assumed as shown in Figure.2. Some of these modes are enumerated below:

(1) All power sources (grid, battery, PV) provide power to the load;

(2) PV generation and the grid provide power to the load and charge the battery at the same time.

(3) PV generation solely supports the load and charges the battery. No power is needed from the grid.

(4) PV generation and batteries support the load together. No power is needed from the grid.

(5) PV generation and batteries support the load and their extra power flows back to the grid.

(6) The grid and the battery together support the load and the power generated from PV is negligible.

Instead of analyzing these operational modes individually, this project proposes a simpler method to control and manage the flow of power, which will be discussed in the coming chapters.

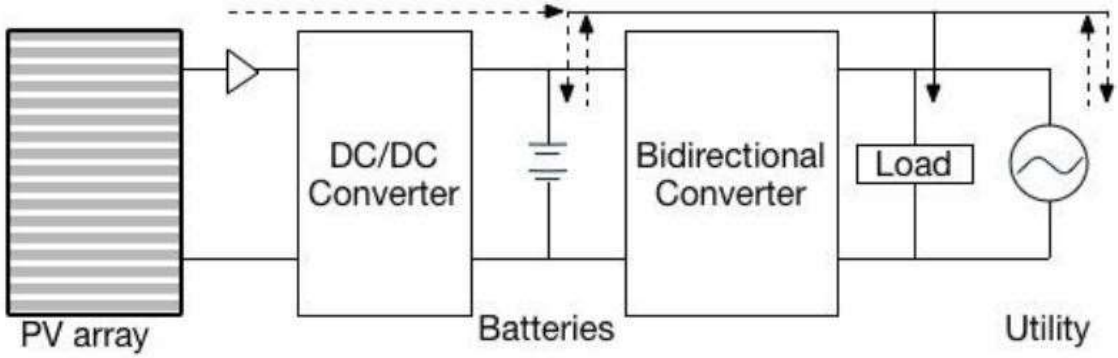

Figure 3.6

Power Flow Equation $P_{pv} \pm P_{BESS} = P_{grid}$

Mode of Operation

Mode 1: PV supplying load and charging battery $P_{pv} = P_{grid} + P_{BESS}$

Mode 2: PV supplying load only $P_{pv} = P_{grid}$

Mode 3: Battery supplying load $P_{BESS} = P_{grid}$

Mode 4: PV-battery both supplying the load $P_{pv} + P_{BESS} = P_{grid}$

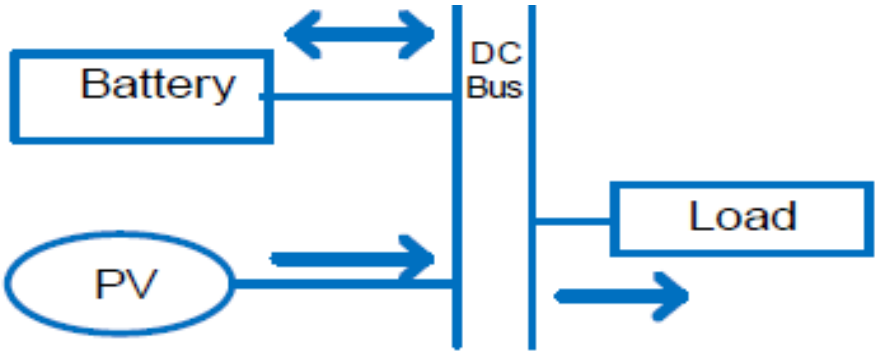

Figure 3.7.

3.6 State-Space Model of PV+BESS

In order to achieve the discharging and charging modes of the battery, the DC/DC converter must be bidirectional. The bidirectional DC/DC converter consists of an inductance Lac, a capacitance Cdc , two diodes D_1 and D_2 with two switches S_1 and S_2, as shown in the DC/DC converter part in Figure 4.

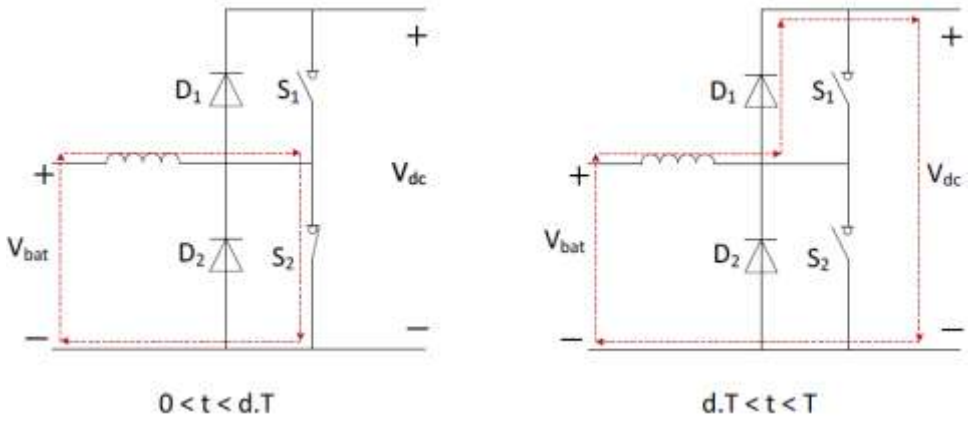

$$V_{bat} = (1-d)V_{dc}$$

Figure 3.8.

As show in Figure 5, S_1 is kept open in the discharging mode of the battery, and S_2 switch opens and closes by the duty ratio *d (0<d<1)*. *T* is the time period that S_2 switches. When $0 < t < d.T$, S_2 is closed, and we have:

$$-V_{bat} = L_{dc}\frac{dI_{bat}}{dt} \quad .....(1)$$

When $dT < t < T$, S_2 is opened, and we have:

$$V_{dc} - V_{bat} = L_{dc}\frac{dI_{bat}}{dt} \quad .....(2)$$

We notice that after the system reaches steady state, the average of current through inductance Lac should be constant. Therefore, we have:

$$\int_0^{d.T} \left(V_{dc} - V_{bat}\right) dt = \int_{d.T}^{T} \left(-V_{bat}\right) dt \quad .....(3)$$

Integrating both sides of (3), and rewriting the equation in terms of Vbat, we get:

$$V_{bat} = \frac{(1-d).T}{T.V_{dc}} = (1-d)V_{dc} \quad .....(4)$$

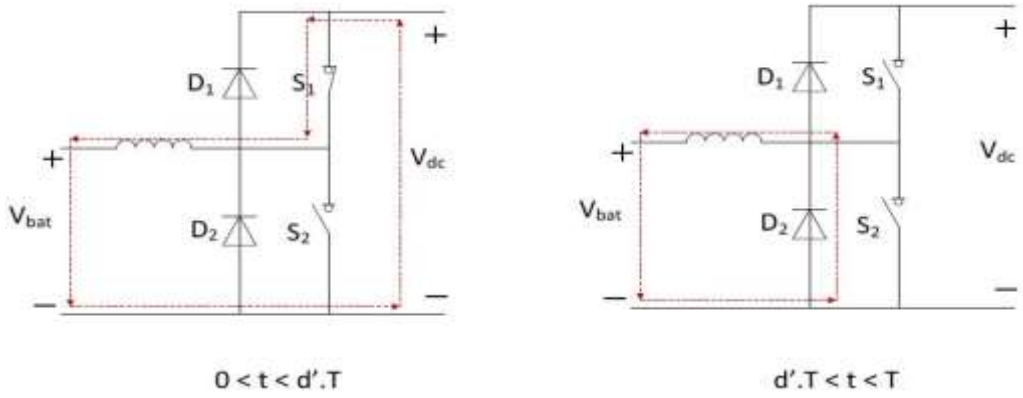

$$V_{bat} = d'.V_{dc}$$

Figure 3.9.

As shown in Figure 6, in battery charging mode, S_2 keeps open and S_1 switches. Assuming the duty ratio in charging mode is *d',* when $0 < t < d'.T$, S_1 is closed, then we have:

$$L_{dc}\frac{dI_{bat}}{dt} = V_{dc} - V_{bat} \quad ....(5)$$

When $d'T < t < T$, S_1 is open, and we have:

$$L_{dc}\frac{dI_{bat}}{dt} = -V_{bat} \quad .....(6)$$

Same as discharging mode, we can have:

$$\int_0^{d'.T} V_{bat}\, dt = \int_{d'.T}^{T} \left(V_{dc} - V_{bat}\right) dt \quad .....(7)$$

Integrating both sides of (7), and writing the equation in terms of Vbat, we can get:

$$V_{bat} = d'V_{dc} \quad ....(8)$$

Comparing equations (4) and (8), for having the same duty ratio in the charging and discharging modes of the DC/DC converter, we set:

$$d = 1 - d' \text{.....(9)}$$

Then we can write both equations (4) and (8) as:

$$V_{bat} = (1-d)V_{dc} \text{ .....(10)}$$

Assuming the DC/DC converter to be lossless, we can express the relation between Idc and Ibat in steady-state as:

$$I_{dc} = (1-d)I_{bat} \text{ .....(11)}$$

AC/DC Rectifier

On the grid and AC/DC converter side, through KVL we get:

$$-V_{abc} + L_{ac}\frac{dI_{abc}}{dt} + e_{abc} = 0 \text{ ....(12)}$$

Assuming the AC/DC converter to be lossless, and equalizing the power on the two sides, we can get:

$$-V_a I_a - V_b I_b - V_c I_c = C_{dc}.V_{dc}.\frac{dV_{dc}}{dt} + \frac{V_{dc}^{\ 2}}{R_{dc}} + V_{dc}I_{dc} \text{ .....(13)}$$

Assuming the DC/DC converter to be lossless, power will be the same on its both sides. As a result:

$$I_{dc} = V_{bat}.I_{bat}/V_{dc} \text{ .....(14)}$$

Transforming the *abc* stationary reference frame in the above equations to the *dq* reference frame rotating at synchronous speed we get:

$$X_{dq0} = \left(\frac{2}{3}\right)\begin{bmatrix} \cos\theta & \cos(\theta-120^0) & \cos(\theta+120^0) \\ -\sin\theta & -\sin(\theta-120^0) & -\sin(\theta+120^0) \\ \frac{1}{2} & \frac{1}{2} & \frac{1}{2} \end{bmatrix} X_{abc} \text{ ....(15)}$$

Where $\theta = \omega t + \theta_0$

Equation (12) can be written in the *dq* reference frame as:

$$\frac{dI_d}{dt} = \omega I_q + \frac{1}{L_{ac}}(V_d - e_d) \text{ .....(16)}$$

$$\frac{dI_q}{dt} = -\omega I_d + \frac{1}{L_{ac}}(V_q - e_q) \text{ .....(17)}$$

Neglecting the harmonics and assuming a sinusoidal pulse width modulation of the AC/DC converter, Vd and Vq can be written as:

$$V_d = 0.5k.V_{dc}\cos(\theta_0 + \alpha) \text{ .....(18)}$$

$$V_q = 0.5k.V_{dc}\sin(\theta_0 + \alpha) \text{ .....(19)}$$

where *k* and alpha are modulation amplitude and angle, respectively

By substituting (18) and (19) into (16) and (17), we get:

$$\frac{dI_d}{dt} = \omega I_q + \frac{1}{L_{ac}}\left(0.5k.V_{dc}\cos\left(\theta_0+\alpha\right) - V_m\cos\theta_0\right) \text{.....(20)}$$

$$\frac{dI_q}{dt} = -\omega I_d + \frac{1}{L_{ac}}\left(0.5k.V_{dc}\sin\left(\theta_0+\alpha\right) - V_m\sin\theta_0\right) \text{.....(21)}$$

We can also rewrite equation (13) by transforming the stationary *abc* reference frame to the rotating *dq* frame, and as a result:

$$\frac{dV_{dc}}{dt} = -\frac{1}{C_{dc}}\left[\frac{3}{4}k\cos\left(\theta_0+\alpha\right)I_d + \frac{3}{4}k\sin\left(\theta_0+\alpha\right)I_q + \frac{V_{dc}}{R_{dc}} + I_{dc}\right] \text{.....}(22)$$

State Space Modeling Function

In this project, by using the Thevenin battery model, we find five state variables for the battery energy storage system, including Id ,Iq ,Vdc , and Ibat the voltage of the capacitor inside the Thevenin battery model Vt, which is related to the battery's current through the following differential equation:

$$\frac{dI_{bat}}{dt} = \frac{1}{L_{dc}}\left(\left(1-d\right)V_{dc} - V_t - R_0.I_{bat} - E_0\right) \text{.....}(23)$$

where Eo is the voltage of the voltage source inside the Thevenin battery model. The differential equation for Vt is written as:

$$\dot{V_t} = \frac{1}{C_t}\left(I_{bat} - \frac{V_t}{R_t}\right) \text{.....}(24)$$

In summary, we can express equations (20) to (24) in state-space form as follows:

$$\dot{X} = F\left(X\right) + G\left(X\right)U \quad \text{.....}(25)$$

where:

$$X = \begin{bmatrix} I_{bat} & V_{dc} & I_d & I_q & V_t \end{bmatrix}^T \text{.....}(26)$$

$$F\left(X\right) = \begin{bmatrix} \dfrac{-V_t - R_0.I_{bat} - E_0}{L_{dc}} \\ -\dfrac{V_{dc}}{R_{dc}.C_{dc}} \\ +\omega I_q - \dfrac{e_d}{L_{ac}} \\ -\omega I_d - \dfrac{e_q}{L_{ac}} \\ \dfrac{1}{C_t}\left(I_{bat} - \dfrac{V_t}{R_t}\right) \end{bmatrix} \text{.....}(27)$$

$$G(X)=\begin{bmatrix} \frac{V_{dc}}{L_{dc}} & 0 & 0 \\ -\frac{I_{bat}}{C_{dc}} & -\frac{3}{2}\cdot\frac{I_d}{C_{dc}} & -\frac{3}{2}\cdot\frac{I_q}{C_{dc}} \\ 0 & \frac{V_{dc}}{L_{ac}} & 0 \\ 0 & 0 & \frac{V_{dc}}{L_{ac}} \\ 0 & 0 & 0 \end{bmatrix} \quad .....(28)$$

$$U=\begin{bmatrix}(1-d) & U_d & U_q\end{bmatrix}^T \quad .....(29)$$

$$U_d = 0.5k\cos(\theta_0+\alpha) \quad .....(30)$$

$$U_q = 0.5k\sin(\theta_0+\alpha) \quad .....(31)$$

Chapter 4

Three-Phase Grid Connected VSI

4.1 Inverter Topology

PV inverter, which is the heart of a PV system, is used to convert dc power obtained from PV modules into ac power to be fed into the grid. PV arrays are connected to the inverter through a dc-dc boost converter. Improving the output waveform of the inverter reduces its respective harmonic content and, hence, the size of the filter used and the level of electromagnetic interference (EMI) generated by switching operation of the inverter . In recent years, multilevel inverters have become more attractive for researchers and manufacturers due to their advantages over conventional three-level pulsewidth-modulated (PWM) inverters. They offer improved output waveforms, smaller filter size, lower EMI, lower total harmonic distortion (THD) [16]. The three common topologies for multilevel inverters are as follows:

1) diode clamped (neutral clamped)

2) capacitor clamped (flying capacitors)

3) cascaded H-bridge inverter

4.2. Selection Of Inverter

The cascaded H-Bridge multilevel inverter are the most advanced and important method of power electronic converters

that analyses output voltage with number of dc sources as inputs. As compared to neutral point clamped multilevel inverter and flying capacitor multilevel inverter, the cascaded H-Bridge multilevel inverters requires less number of components and it reaches high quality output voltage which is close to sinewave. By increasing the number of output levels the total harmonic distortion in output voltage can be reduced. Multilevel inverter

offers less total harmonic distortion compared to the conventional H-Bridge inverters. Increasing level leads to less harmonic distortion,but increasing levels also increase switching loss which reduces efficiency.

Voltage source inverter(VSI) is used in case of constant DC voltage input. Current source inverter(CSI) is used where input current remains constant. In our case, we are dealing with constant dc voltage, which is maintained by dc-dc boost converter. Also, in case of high frequency switching VSI is used. Semiconductor switching devices of inverter are controlled by PWM signals to obtain three phase near sinusoidal ac voltages of desired magnitude and frequency at the inverter output.[17]

4.3. Operation

The three-phase dc/ac voltage source inverters are extensively being used in motor drives, active filters and unified power flow controllers in power systems and uninterrupted power supplies to generate controllable frequency and ac voltage magnitudes using various pulse width modulation (PWM) strategies. The standard three-phase inverter shown in Figure 4.1 has six switches the switching of which depends on the modulation scheme. The input dc is usually obtained from the dc-dc boost converter.

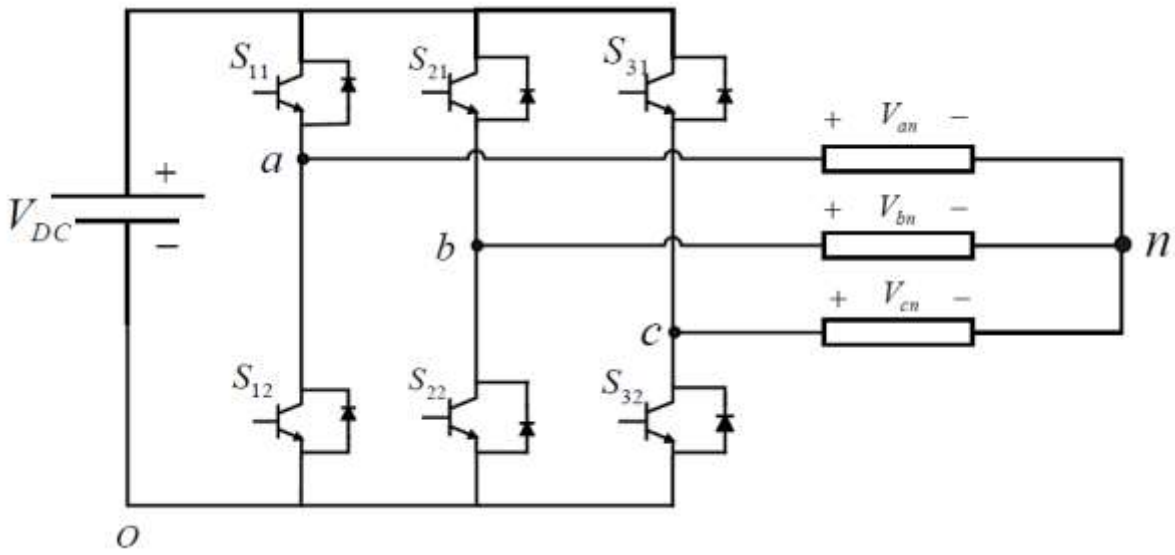

Fig 4.1: Three-phase Full –Bridge Inverter

The inverter has eight switch states given in Table 4.1. As explained earlier in order that the circuit satisfies the KVL and the KCL, both of the switches in the same leg cannot be turned ON at the same time, as it would short the input voltage violating the KVL. Thus the nature of the two switches in the same leg is complementary. In accordance to Figure 4.1,

$$S_{11} + S_{12} = 1 \quad \text{.....(4.3.1)}$$

$$S_{21} + S_{22} = 1 \quad \text{.....(4.3.2)}$$

$$S_{31} + S_{32} = 1 \quad \text{.....(4.3.3)}.$$

S_{11}	S_{12}	S_{31}	V_{ab}	V_{bc}	V_{ca}
0	0	0	0	9	0
0	0	1	0	$-V_{DC}$	V_{DC}
0	1	0	$-V_{DC}$	V_{DC}	0
0	1	1	$-V_{DC}$	0	$-V_{DC}$

1	0	0	V_{DC}	0	$-V_{DC}$
1	0	1	V_{DC}	$-V_{DC}$	0
1	1	0	0	V_{DC}	$-V_{DC}$
1	1	1	0	0	0

Table 4.1: The switching states in a three-phase inverter

Of the eight switching states as shown in Table 4.1 two of them produce zero ac line voltage at the output. In this case, the ac line currents freewheel through either the upper or lower components. The remaining states produce no zero ac output line voltages. In order to generate a given voltage waveform, the inverter switches from one state to another. Thus the resulting ac output line voltages consist of discrete values of voltages, which are $-V_{DC,}$ 0, and $V_{DC.}$

The selection of the states in order to generate the given waveform is done by the modulating technique that ensures the use of only the valid states**.**

$$\frac{V_{DC}}{2}(S_{11}-S_{12})=V_{an}+V_{no} \quad \text{.....(4.3.4)}$$

$$\frac{V_{DC}}{2}(S_{21}-S_{22})=V_{bn}+V_{no} \quad \text{.....(4.3.5)}$$

$$\frac{V_{DC}}{2}(S_{31}-S_{32})=V_{cn}+V_{no} \quad \text{.....(4.3.6)}$$

Expressing the Equations from 4.3.4 to 4.3.6 in terms of modulation signals and making use of conditions from 4.3.1 to 4.3.3 gives

$$\frac{V_{DC}}{2}(M_{11})=V_{an}+V_{no} \quad \text{.....(4.3.7)}$$

$$\frac{V_{DC}}{2}(M_{21})=V_{bn}+V_{no} \quad \text{.....(4.3.8)}$$

$$\frac{V_{DC}}{2}(M_{31})=V_{cn}+V_{no} \quad \text{.....(4.3.9)}$$

Adding the Equations from 4.3.4 to 4.3.6 together gives Equation 4.3.10 as

$$\frac{V_{DC}}{2}(S_{11}+S_{21}+S_{31}-S_{12}-S_{22}-S_{32})=V_{an}+V_{bn}+V_{cn}+3V_{no} \quad \text{.....(4.3.10)}$$

As we are dealing with balanced voltages $V_{an}+V_{bn}+V_{cn}=0$ and making use of the conditions from Equations 4.1 to 4.3, Equation 4.3.10 becomes

$$\frac{V_{DC}}{6}(2S_{11}+2S_{21}+2S_{31}-3)=V_{no} \quad \text{.....(4.3.11)}$$

Substituting for Vin Equations 4.3.4 to 4.3.6, gives

$$\frac{V_{DC}}{3}(2S_{11}-S_{21}-S_{31})=V_{an} \quad \text{.....(4.3.12)}$$

$$\frac{V_{DC}}{3}(2S_{21}-S_{21}-S_{31})=V_{bn} \quad \text{.....(4.3.13)}$$

$$\frac{V_{DC}}{3}(2S_{31}-S_{21}-S_{11})=V_{cn} \quad \text{.....(4.3.14)}$$

4.4. State-space representation

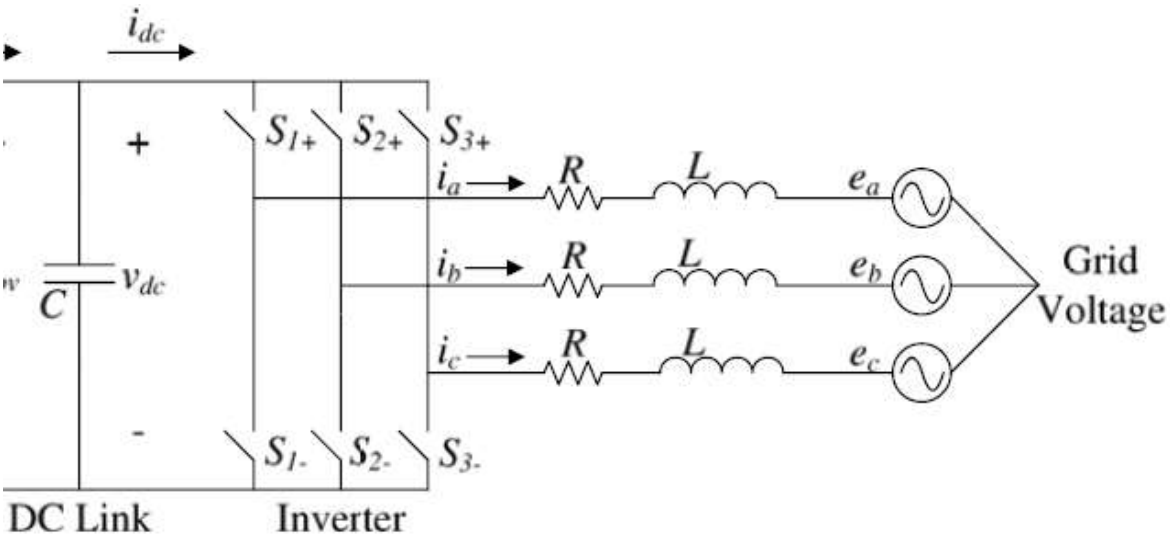

Fig 4.2: Three-phase grid-connected inverter

a state-space representation is a mathematical model of a physical system as a set of input, output and state variables related by first-order differential equations or difference equations.In state-space form, the system in Fig. 1 can be represented
by the following equations

$$\dot{i_a} = -\frac{R}{L} i_a - \frac{1}{L} e_a + \frac{v_{pv}}{3L}(2K_a - K_b - K_c)$$
$$i_b = -\frac{R}{L} i_b - \frac{1}{L} e_b + \frac{v_{pv}}{3L}(-K_a + 2K_b - K_c)$$
$$\dot{i_c} = -\frac{R}{L} i_c - \frac{1}{L} e_c + \frac{v_{pv}}{3L}(-K_a - K_b + 2K_c) \qquad (4.4.1)$$

Where K_a, K_b and K_c are the input switching signals. Now, by
applying KCL at the node where the dc link is connected, we get-

$$\dot{v_{pv}} = \frac{1}{C}(i_{pv} - i_{dc}) \qquad (4.4.2)$$

However, the input current of the inverter i_{dc} can be written
as

$$i_{dc} = i_a K_a + i_b K_b + i_c K_c \qquad (4.4.3)$$

which yields

$$\dot{v_{pv}} = \frac{1}{C} i_{pv} - \frac{1}{C}(i_a K_a + i_b K_b + i_c K_c) \qquad (4.4.4.)$$

The complete model of a three-phase grid-connected PV can
be presented by (4.4.1) and (4.4.4) which are nonlinear and time varying.This time-varying model can be converted into time-invariant model by applying *dq* transformation.[2]

4.5. Park transformation

Park transformation is needed to reduce complexity of the system with dc values instead of ac values.DQ frame allows system to be controlled by one controller for only d axis. The Park transform converts vectors in the XYZ reference frame to the *DQ* reference frame. The primary value of the Park transform is to rotate the reference frame of a vector at an arbitrary frequency. The Park transform shifts the frequency spectrum of the signal such that the

arbitrary frequency now appears as "dc" and the old dc appears as the negative of the arbitrary frequency. The Park transformation matrix is

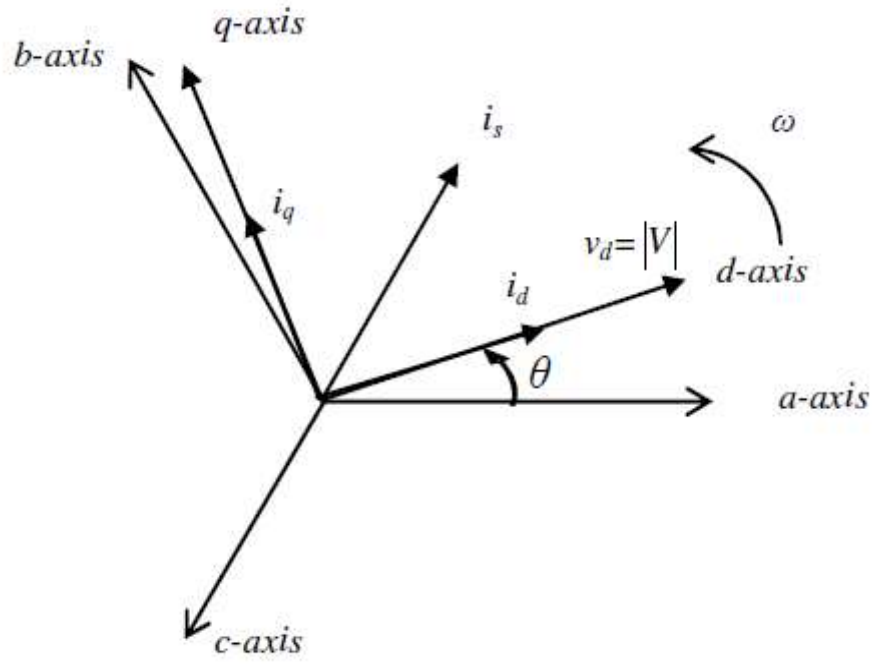

Fig 4.3:abc to dq frame

$$[T_{dq0}(\theta)] = \frac{2}{3}\begin{bmatrix} \cos\theta & \cos\left(\theta-\frac{2\pi}{3}\right) & \cos\left(\theta+\frac{2\pi}{3}\right) \\ -\sin\theta & -\sin\left(\theta-\frac{2\pi}{3}\right) & -\sin\left(\theta+\frac{2\pi}{3}\right) \\ \frac{1}{2} & \frac{1}{2} & \frac{1}{2} \end{bmatrix}$$

Abc to dq transformation equation

$$[I_{dq0}] = [T_{dq0}(\theta)][i_{abc}]$$

This time-varying model can be converted into time-invariant model by applying dq transformation [15] using the angular frequency ω of the grid, rotating reference frame synchronized with grid where the d component of the grid voltage Ed is zero [ref15], [ref19]. By using dq transformation, (4.4.1) and (4.4.4) can be written as

$$\dot{I}_d = -\frac{R}{L}I_d + \omega I_q - \frac{E_d}{L} + \frac{v_{pv}}{L}K_d$$

$$\dot{I}_q = -\omega I_d - \frac{R}{L}I_q - \frac{E_q}{L} + \frac{v_{pv}}{L}K_q$$

$$\dot{v_{pv}} = \frac{1}{C} i_{pv} - \frac{1}{C} I_d K_d - \frac{1}{C} I_q K_q$$

These three equations represents the complete mathematical model of the three-phase grid-connected PV system, which is nonlinear due to the switching functions and diode current. K_d and K_q are the control inputs, and the output variables are I_q .

and v_{pv}.

4.6. Filter

Normally, VSIs are connected to the grid using *L* or *LC* filter, but at low frequencies the *L* (Inductor) and *LC* (Inductor Capacitor) filters becomes bulky and expensive. So, to reduce the cost and the size parameters, the *LCL* filter was introduced[ref].Grid-connected inverter requires an output low-pass filter to interface with the grid for harmonics attenuations, better output response. LCL filter is popular now-a-days for grid connected VSI. Due to simplicity in state-space representation we used L-filter.As LCL requires more steps which will lead to complex calculation.[18]

Chapter 5

Stability Analysis Of Grid Connected PV+BESS

5.1 Definition

Over the years, several definitions of power systems stability have been formulated aiming at clarifying technical and physical aspects of the problem from the system theory perspective. The stability concert more consistent with the emphasis placed in this research work is the one relating to the system's ability to ride-through disturbances arising the system itself and its capacity to

settle down to a new stable operating state after the effects of such disturbance disappears. A formal definition of power system stability is provided by [96-98].

"Power system stability is the ability of an electric power system, for a given initial operating condition, to regain a state of operating equilibrium after being subjected to a physical disturbance, with most system variables bounded so that practically the entire system remains intact."

The power system is a highly nonlinear system that operates in a constantly changing environment;loads, generator outputs and key operating parameters change continually. When subjected to a disturbance, the stability of the system depends on the initial operating condition as well as the nature of the disturbance.

5.2 General Categories Of Stability

The classification of power system stability proposed here is based on the following considerations [98]:

- The physical nature of the resulting mode of instability as indicated by the main system variable in which instability can be observed.

The size of the disturbance considered, which influences the method of calculation and prediction of stability.

- The devices, processes, and the time span that must be taken into consideration in order to assess stability.

Figure (1) gives the overall picture of the power system stability problem, identifying its categories and subcategories. The following are descriptions of the corresponding forms of stability phenomena.

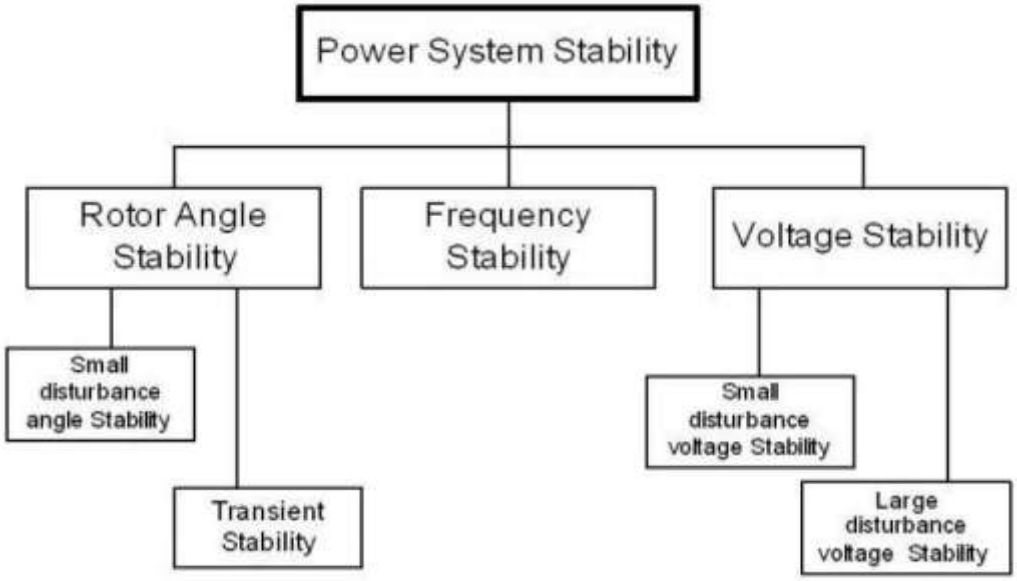

Fig 5.1

Transient stability

Transient stability is concerned with the system's ability to maintain synchronism following a large or severe disturbance. Unlike small-signal stability, transient stability is analyzed by studying and simulating how the system responds in the time domain. The transient stability of the system depends on both the initial operating conditions of the system and the severity of the disturbance, in general the transient stability is defined as, the capability of a power system to return to a stable operating point after the occurrence of a disturbance that changes its topology.

Small signal stability

Small signal stability is defined as the capability of the power system to return to a stable operating point after the occurrence of a disturbance that leads to an incremental change in one or more of the state variables of the power system.

Whereas the definition of small signal stability refers to the system's response to a small change in one or more of its state variables. The disturbances are considered to be sufficiently small that linearization of system equations is permissible for purposes of analysis [97-98, 2, 111].

Examples of state variables of a power system are:

- synchronous and asynchronous machine rotor speeds
- synchronous machine load angles
- magnetic flux linkages
- controller state variables

If a disturbance causes a change in the value of one or more of these state variables, the system is driven from the equilibrium. If thereafter the system returns to its steady state, it is stable, whereas if the initial deviation from the steady state becomes ever larger, it is unstable. A further difference between transient stability and small signal stability is that if a steady state is reached after a disturbance leading to a transient phenomenon, i.e. a change in the system's topology, the new steady state can be different from the initial one. In contrast, if a system returns to a steady state after an incremental change in a state variable, this steady state is identical to the initial steady state, because no change in the network's topology has occurred.

5.3 Linearizartion Using Taylor's Series

The dynamic response of a power system subject to small disturbances can be studied by using the method introduced in Chap. 7 to determine system stability.However, when we use the method for power system small-signal stability analysis, in addition to slow computational speed, the weakness is that after a conclusion of instability is drawn, we cannot carry out any deeper investigation into the phenomenon and cause of system instability. The Lyapunov linearized method has provided a very useful tool for power system small-signal stability analysis. Based on the fruitful results of eigensolution analysis of linear systems, the Lyapunov linearized method has been widely used in power system small-signal stability analysis. In the following, we shall first introduce the basic mathematics of power system small-signal stability analysis.The Lyapunov linearized method is closely related to the local stability of nonlinear systems. Intuitively speaking, movement of a nonlinear system over a small range should have similar properties to its linearized approximation.

Assume the nonlinear system described by

$$\frac{\mathrm{d}\mathbf{x}}{\mathrm{d}t} = f(\mathbf{x}).$$

Its Taylor expansion at the origin is

$$\frac{\mathrm{d}\Delta\mathbf{x}}{\mathrm{d}t} = \mathbf{A}\Delta\mathbf{x} + \mathbf{h}(\Delta\mathbf{x})$$

Where

$$\mathbf{A} = \left.\frac{\partial \mathbf{f}(\mathbf{x}_e + \Delta\mathbf{x})}{\partial \Delta\mathbf{x}}\right|_{\Delta\mathbf{x}=\mathbf{0}} = \left.\frac{\partial \mathbf{f}(\mathbf{x})}{\partial \mathbf{x}}\right|_{\mathbf{x}=\mathbf{x}_e}$$

If in the neighborhood of Dx = 0, h(Dx) is a high-order function of Dx, we can use the stability of the following linear system

$$\frac{d\Delta \mathbf{x}}{dt} = \mathbf{A}\Delta \mathbf{x}$$

To study the stability of the nonlinear system at point xe

(1) If the linearized system is asymptotically stable, i.e., all eigenvalues of A have negative real parts, the actual nonlinear system is asymptotically stable at the equilibrium point.

(2) If the linearized system is unstable, i.e., at least one of eigenvalues of A has a positive real part, the actual nonlinear system is unstable at the equilibrium point.

(3) If the linearized system is critically stable, i.e., real parts of all eigenvalues of A are nonpositive but the real part of at least one of them is zero, no conclusion can be drawn about the stability of the nonlinear system from its linearized approximation. The basic principle of the Lyapunov linearized method is to draw conclusions about

the local stability of the nonlinear system around the equilibrium point from the stability of its linear approximation.

When carrying out small-signal stability analysis of a power system, we always assume that the system at normal operation at equilibrium point x ¼ xe or Dx ¼ 0 is disturbed instantly at the moment t ¼ t0 when system state moves from 0 to Dx(t0). Dx(t0) is the initial state of system free movement after disappearance of the disturbance. Because the disturbance is sufficiently small, Dx(t0) is within a sufficiently small neighborhood of Dx ¼ 0. Thus in the neighborhood of Dx ¼ 0, h(Dx) is a high-order indefinitely small variable. Hence according to the Lyapunov linearized method, we can study the stability of the linearized system to investigate that of the actual nonlinear power system.

Fig 5.3 subcarrier mapping schemes of Non Binary Octal SC_FDMA

5.4 Characteristics Of Small Signal Stability

Small signal stability problems may be either local or global in nature. Local problems involve a small part of the power system, and are usually associated with rotor angle oscillations of a single power plant against the rest of the power system. Such oscillations are called local plant mode

oscillations. Stability (damping) of these oscillations depends on the strength of the transmission system as seen by the power plant, generator excitation control systems and plant output [97-98, 112].

Global problems are caused by interactions among large groups of generators and have widespread effects. They involve oscillations of a group of generators in one area swinging against a group of generators in another area. Such oscillations are called inter-area mode oscillations. Their characteristics are very complex and significantly differ from those of local plant mode oscillations. Load characteristics, in particular, have a major effect on the stability of inter-area modes [97- 98].

The time frame of interest in small-disturbance stability studies is on the order of 10 to 20 seconds following a disturbance.

5.5 Initial Value Calculation

$$\frac{dI_{pv}}{dt} = -(1-D)\frac{V_{dc}}{L} + \frac{V_{pv}}{L}$$

$$\frac{dV_{dc}}{dt} = (1-D)\frac{i_{pv}}{C_1} - \frac{V_{dc}}{R_1 C_1}$$

$$\frac{dI_d}{dt} = \omega I_q - \frac{e_d}{L_{ac}} + \frac{v_{dc}}{L_{ac}} K_d$$

$$\frac{dI_q}{dt} = -\omega I_d - \frac{e_q}{L_{ac}} + \frac{v_{dc}}{L_{ac}} K_q$$

$$\frac{dV_{dc}}{dt} = \frac{I_{dc}}{C_{dc}} - \frac{I_d K_d}{C_{dc}} - \frac{I_q K_q}{C_{dc}}$$

$$\frac{dV_t}{dt} = \frac{I_{bat}}{C_2} - \frac{V_t}{R_2 C_2}$$

$$\frac{dI_{bat}}{dt} = \frac{V_{dc} - V_t - I_{bat} R_o - E_o}{L_{dc}} - \frac{V_{dc}}{L_{dc}} d$$

$$\tan\theta = \frac{Q_{grid}}{P_{grid}}$$

$$P_{grid} = \frac{3}{2} e_d I_d$$

$$Q_{grid} = -\frac{3}{2} e_d I_q$$

$$I_{dc} = (1 - D).I_{pv}$$

5.6 MATLAB Code for Initial Value Calculation

```
clear all;
clc;
%PV Parameters
Vpv=0.1;
Ipv=10.1327;

Rs=0.05;
Rsh=100;
Ns=60;
Np=1;
A=1.3;
k=1.38e-23;
T=298;
Is=2.8393e-10;
q=1.6e-19;
alpha=q/(A*k*T);

% Parameters for Linearization of Ipv
M=(Vpv/Ns)+(Ipv*Rs)/Np;
Z1=Is*alpha*Rs*exp(alpha*M)+Rs/Rsh;
Z2=-(Np/Ns)*alpha*Is*exp(alpha*M)-Np/(Rsh*Ns);

% Dc-Dc Boost
R1=20;
C1=10*10^(-6);
L=1*10^(-3);

%BDC
Lac=.1098*10^(-3);
Cdc=.05*10^(-6);
Ldc=.755*10^(-3);
C2=80;
R2=0.07;
R0=0.0207;
d=0.5;
Q=300;

%Grid
ed=230;
Pgrid=10000;
theta=pi/6;
```

```
eq=0;
f=60;
w=2*3.14*f;

%Equations under Steady State operations
Vdc=sqrt(Vpv*Ipv*R1);
D=1-Vdc/(Ipv*R1);
Id=Pgrid/(1.5*ed);
Idc=(1-D)*Ipv;
Kq=(w*Lac*Id)/Vdc;
Ibat=Idc/(1-d);
Vt=Ibat*R2;
E0 = Vdc*(1 - d)-Vt-(Ibat*R0);
Qgrid=(Pgrid*tan(theta));
Iq=-(2*Qgrid)/(3*ed);
Kd=(((ed/Lac)-w*Iq*Lac)/Vdc);
```

Parameters	Values	Parameters	Values	Parameters	Values
Vpv	0.1 V	C2	80 F	w	376.8
Ipv	10.13 A	R2	0.07 ohm	Vdc	4.5 V
Iq	-16.73 A	Ro	0.02 ohm	D	0.9
Kd	4.6e5	d	0.5	Id	28.98 A
R1	20 ohm	Q	300	Idc	0.22 A
C1	10e-5 F	ed	230	Kq	0.26
L	10e-3 H	Pgrid	10e3	Ibat	0.45 A
Lac	10e-4 H	θ	Pi/6	Vt	0.03 V
Cdc	10e-6 F	eq	0	Eo	2.21
Ldc	10e-3 H	f	60 Hz	Qgrid	5.7e3

5.7 Eigenvalues and Small Signal Stability

The main goal of this section is to figure out the correspondence between the eigenvalues of an electrical power system and its dynamic characteristics. First the linearization of the state equations

of the power system will be discussed. After that, the correspondence between the eigenvalues of the state matrix which is the crucial part of the linearized description, and the time domain will be pointed out.

Eigenvalue is a scalar associated with a given linear transformation of a vector space and having the property that there is some nonzero vector which when multiplied by the scalar is equal to the vector obtained by letting the transformation operate on the vector; *especially* it is the root of the characteristic equation of a matrix.

Modal Analysis

In this thesis the focus will be on modeling of wind turbine connected to DFIG, which can be described by a set of *n* First-order non-linear, ordinary algebraic-differential equations (DEA) of the following form [98, 112-113]:

$$\frac{dx_i}{dt} = f_i\left(x_1, x_2, \ldots, x_n; z_1, z_2, \ldots, z_m; u_1, u_2, \ldots, u_r\right)$$

$$0 = g_i\left(x_1, x_2, \ldots, x_n; z_1, z_2, \ldots, z_m; u_1, u_2, \ldots, u_r\right)$$

The mathematical model of a power system can be written as a set of DAE

$$\dot{x} = f\left(x, z, u\right)$$

$$y = g\left(x, z, u\right)$$

With

$$\mathbf{x} = \begin{bmatrix} x_1 \\ x_2 \\ \vdots \\ x_n \end{bmatrix} \quad \mathbf{z} = \begin{bmatrix} z_1 \\ z_2 \\ \vdots \\ z_m \end{bmatrix} \quad \mathbf{u} = \begin{bmatrix} u_1 \\ u_2 \\ \vdots \\ u_r \end{bmatrix} \quad \mathbf{f} = \begin{bmatrix} f_1 \\ f_2 \\ \vdots \\ f_n \end{bmatrix} \quad \mathbf{g} = \begin{bmatrix} g_1 \\ g_2 \\ \vdots \\ g_n \end{bmatrix}$$

Where

f is a vector containing n first-order non-linear differential equations

x is a vector containing n state variables

u is a vector containing r input variables

g is a vector containing n non-linear algebraic equations

z is a vector containing m algebraic variables

y is a vector containing m output variables

By assuming that the system in equation 2.3 is time invariant, i.e. the time derivatives of the state variables are not explicit functions of the time, *t* can be excluded from equation 2.3. In smallsignal analysis, equations 2.3and 2.4 can be linearized by a Taylor series expansion around an operating point (x_0,z_0,u_0) and the resulting linearized description of the system can be used to investigate its response to small variations in the input or state variables, starting at an equilibrium point [98, 114-115].Neglecting the terms of order two and above and eliminating the algebraic variables **z** just taking into account first-order terms ,the system state matrix is obtained from derivations given below. A procedure for small perturbations is established for *ith* component of vector **x** .

$$\dot{x}_i = \dot{x}_{i0} + \Delta\dot{x}_i = f_i\left[(x_0 + \Delta x_0),(u_0 + \Delta u_0)\right]$$

$$= f_i(x_0,u_0) + \frac{\partial f_i}{\partial u_i}\Delta x_i + \ldots + \frac{\partial f_i}{\partial u_n}\Delta x_n + \frac{\partial f_i}{\partial u_1}\Delta u_1 + \ldots + \frac{\partial f_i}{\partial u_r}\Delta u_r$$

From equation (2.3) it follows that

$$\dot{x}_{i0} = f_i(x_0,u_0)$$

And therefore (2.7) can be written as

$$\Delta\dot{x}_i = \frac{\partial f_i}{\partial x_i}\Delta x_i + \ldots + \frac{\partial f_i}{\partial x_n}\Delta x_n + \frac{\partial f_i}{\partial u_1}\Delta u_1 + \ldots + \frac{\partial f_i}{\partial u_r}\Delta u_r$$

With i =1,2,..., n
The same can be done for the jth component of y , with reference to (2.4),

$$\Delta \dot{y}_j = \frac{\partial g_j}{\partial x_1}\Delta x_1 + \ldots + \frac{\partial g_j}{\partial x_n}\Delta x_n + \frac{\partial g_g}{\partial u_1}\Delta u_1 + \ldots + \frac{\partial j_j}{\partial u_r}\Delta u_r$$

With j =1, 2,..., n
The prefix Δ denotes a small deviation, thus

$$\Delta x = x - x_0 \qquad \Delta y = y - y_0 \qquad \Delta u = u - u_0$$

Doing this for all components of the vectors x and y gives the following linearized set of state and output equations

$$\Delta \dot{\mathbf{x}} = \mathbf{A}\Delta \mathbf{x} + \mathbf{B}\Delta \mathbf{u}$$

$$\Delta \mathbf{y} = \mathbf{C}\Delta \mathbf{x} + \mathbf{D}\Delta \mathbf{u}$$

With

$$\mathbf{A} = \begin{pmatrix} \frac{\partial f_1}{\partial x_1} & \cdots & \frac{\partial f_1}{\partial x_n} \\ \vdots & \ddots & \vdots \\ \frac{\partial f_n}{\partial x_1} & \cdots & \frac{\partial f_n}{\partial x_n} \end{pmatrix} \quad \mathbf{B} = \begin{pmatrix} \frac{\partial f_1}{\partial u_1} & \cdots & \frac{\partial f_1}{\partial u_r} \\ \vdots & \ddots & \vdots \\ \frac{\partial f_n}{\partial u_1} & \cdots & \frac{\partial f_n}{\partial u_r} \end{pmatrix}$$

$$\mathbf{C} = \begin{pmatrix} \frac{\partial g_1}{\partial x_1} & \cdots & \frac{\partial g_1}{\partial x_n} \\ \vdots & \ddots & \vdots \\ \frac{\partial g_m}{\partial x_1} & \cdots & \frac{\partial g_m}{\partial x_n} \end{pmatrix} \quad \mathbf{D} = \begin{pmatrix} \frac{\partial g_1}{\partial u_1} & \cdots & \frac{\partial g_1}{\partial u_r} \\ \vdots & \ddots & \vdots \\ \frac{\partial g_m}{\partial u_1} & \cdots & \frac{\partial g_m}{\partial u_r} \end{pmatrix}$$

Thus, the matrices **A**, **B**, **C** and **D** contain the partial derivatives of the functions in **f** and **g** to the state variables **x** and the input variables **u**. Matrix **A** is the state matrix of the system. Equations ((2.11) and (2.12)) can be Laplace transformed to obtain the state equations in the frequency domain. Take the Laplace transform assuming zero initial conditions [2, 113]

$$s\,\Delta x(s) - \Delta x(0) = \mathbf{A}\,\Delta x(s) + \mathbf{B}\,\Delta u(s)$$

$$\Delta\, y(s) = \mathbf{C}\,\Delta x(s) + \mathbf{D}\,\Delta u(s)$$

A solution to the state equations can be obtained by rearranging the upper equation of (2.14) & (2.15) as follows

$$(s\mathbf{I} - \mathbf{A})\Delta x(0) + \mathbf{B}\Delta u(s)$$

I is the identity matrix and the values of s which satisfy

$$\det(s\mathbf{I} - \mathbf{A}) = 0$$

Are known as the eigenvalues of matrix A and equation (6.10) is defined as the characteristic equation of matrix **A**.

5.8 Stability Analysis without Controller

Small signal representation of the entire system

$$\frac{d\Delta i_{pv}}{dt} = \frac{1 + Z_1}{Z_2 L}\Delta i_{pv} - (1 - D)\frac{\Delta V_{dc}}{L}$$

$$\frac{d\Delta V_{dc}}{dt} = (1 - D)\frac{\Delta i_{pv}}{C_1} - \frac{\Delta V_{dc}}{R_1 C_1}$$

$$\frac{d\Delta I_d}{dt} = \omega\Delta I_q - \frac{e_d}{L_{ac}} + \frac{\Delta v_{dc}}{L_{ac}}K_d$$

$$\frac{d\Delta I_q}{dt} = -\omega\Delta I_d - \frac{e_q}{L_{ac}} + \frac{\Delta v_{dc}}{L_{ac}}K_q$$

$$\frac{d\Delta V_t}{dt} = \frac{\Delta I_{bat}}{C_2} - \frac{\Delta V_t}{R_2 C_2}$$

$$\frac{d\Delta I_{bat}}{dt} = \frac{\Delta V_{dc} - \Delta V_t - \Delta I_{bat}R_o - E_o}{L_{dc}} - \frac{\Delta V_{dc}}{L_{dc}}d$$

$$\frac{d\Delta SOC}{dt} = \frac{\Delta I_{bat}}{C_{bat}}$$

5.8.1 MATLAB Code For Stability Analysis without Controller

```
clear all;
clc;
%PV Parameters
Vpv=.1;
Ipv=10.1327;

Rs=0.05;
Rsh=100;
Ns=60;
```

```
Np=1;
A=1.3;
k=1.38e-23;
T=298;
Is=2.8393e-10;
q=1.6e-19;
alpha=q/(A*k*T);

% Parameters for Linearization of Ipv

M=(Vpv/Ns)+(Ipv*Rs)/Np;
Z1=Is*alpha*Rs*exp(alpha*M)+Rs/Rsh;
Z2=-(Np/Ns)*alpha*Is*exp(alpha*M)-Np/(Rsh*Ns);

% Dc-Dc Boost
R1=20;
C1=10*10^(-6);
L=1*10^(-3);

%BDC
Lac=.1098*10^(-3);
Cdc=.05*10^(-6);
Ldc=.755*10^(-3);
C2=80;
R2=0.07;
R0=0.0207;
d=0.5;
Q=300;

%Grid
ed=230;
Pgrid=10000;
theta=pi/6;
eq=0;
f=60;
w=2*3.14*f;

%Equations under Steady State operations
Vdc=sqrt(Vpv*Ipv*R1);
D=1-Vdc/(Ipv*R1);
Id=Pgrid/(1.5*ed);
Idc=(1-D)*Ipv;
Kq=(w*Lac*Id)/Vdc;
Ibat=Idc/(1-d);
Vt=Ibat*R2;
E0 = Vdc*(1 - d)-Vt-(Ibat*R0);
Qgrid=(Pgrid*tan(theta));
```

```
Iq=-(2*Qgrid)/(3*ed);
Kd=(((ed/Lac)-w*Iq*Lac)/Vdc);

%x1=Ipv; x2=Vdc; x3=Id; x4=Iq; x5=Vt; x6=Ibat; x7=SoC;


syms x1 x2 x3 x4 x5 x6 x7;

f1(x1,x2)=((1+Z1)/(Z2*L))*x1-((1-D)/L)*x2;
f2(x1,x2)=((1-D)/C1)*x1-x2/(R1*C1);
f3(x2,x4)=w*x4-(ed/Lac)+(Kd*x2)/Lac;
f4(x3,x2)=-w*x3-(eq/Lac)+(Kq*x2)/Lac;
f5(x5,x6)=(x5/C2)-x6/(R2*C2);
f6(x2,x5,x6)=((x2-x6-x5*R0-E0)/Ldc)-(x2*d)/Ldc;
f7(x5)=x5/Q;


a(x1,x2,x3,x4,x5,x6,x7) =
jacobian([f1(x1,x2);f2(x1,x2);f3(x2,x4);f4(x3,x2);f5(x5,x6);f6
(x2,x5,x6);f7(x5)], [x1,x2,x3,x4,x5,x6,x7]);
A=vpa(a)
 B=eig(A)
 plot(real(B),imag(B),'r*')
%  J=vpa(B,4)
```

5.8.2 Stability Mode Analysis using Eigenvalue

Eigenvalue	Effect on system when disturbed
Positive real number	Driven away from steady-state value
Negative real number	Driven back to steady-state value
0	Remains at position to which it was disturbed
Identical to another eigenvalue	Effects can not be determined
Complex, positive real number	Oscillates around steady-state value with increasing amplitude
Complex, negative real number	Oscillates around steady-state value with decreasing amplitude
Imaginary	Oscillates around steady-state value with constant amplitude

Modes	Eigen Value	State Condition
λ_1	0.0162	Unstable
λ_2	5.471e-51	Unstable
λ_3	-3.67e-40+376.8i	Stable
λ_4	-3.67e-40-376.8i	Stable
λ_5	-1325	Stable
λ_6	-4004+3368i	Stable
λ_7	-4004-3368i	Stable

5.8.3 Eigen Root-locus without Controller

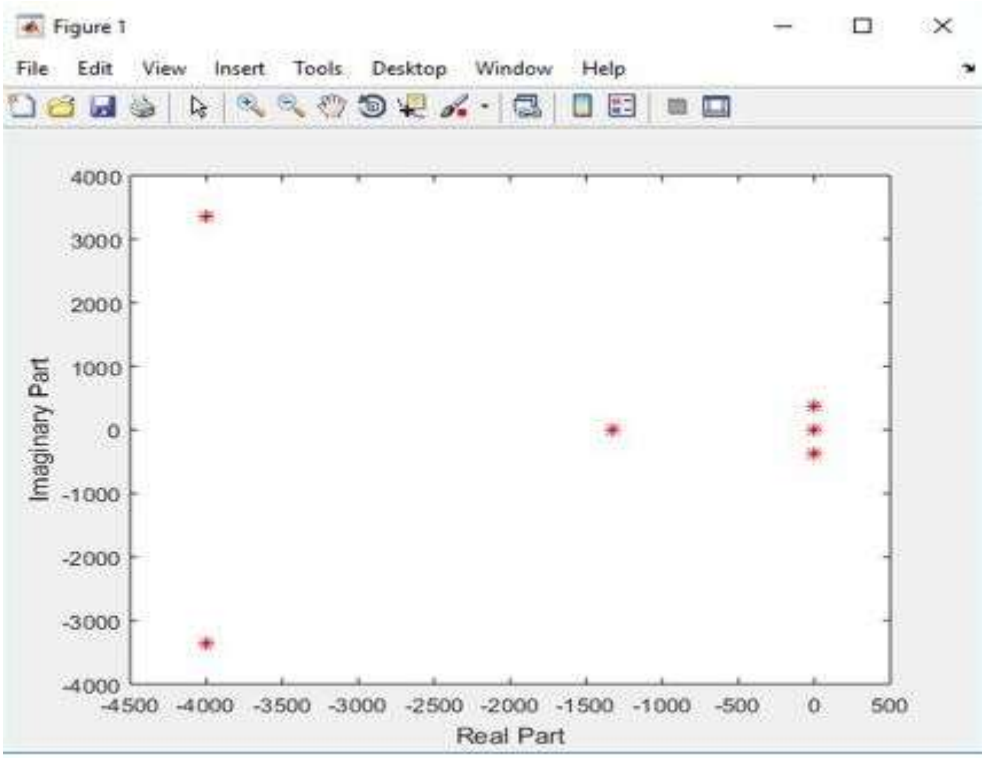

Without Controller

5.9 Stability Analysis with Controller

5.9.1 Proposed PI Controller

Proportional Integral (PI) Controller

At present, the PI controller is most widely adopted in industrial application due to its simple structure, easy to design and low cost. Despite these advantages, the PI controller fails when the controlled object is highly nonlinear and uncertain. PI controller will eliminate forced oscillations and steady state error resulting in operation of on-off controller and P controller respectively. However, introducing integral mode has a negative effect on speed of the response and

overall stability of the system. Thus, PI controller will not increase the speed of response. It can be expected since PI controller does not have means to predict what will happen with the error in near future. This problem can be solved by introducing derivative mode which has ability to predict what will happen with the error in near future and thus to decrease a reaction time of the controller. PI controllers are very often used in industry, especially when speed of the response is not an issue. A control without D mode is used when

1. Fast response of the system is not required
2. Large disturbances and noise are present during operation of the process
3. There is only one energy storage in process (capacitive or inductive)
4. There are large transport delays in the system.

Therefore, we would like to keep the advantages of the PI controller. This leads to propose a PI controller shown in Fig. 6. This controller uses of the proportional term while the integral term is kept, unchanged.

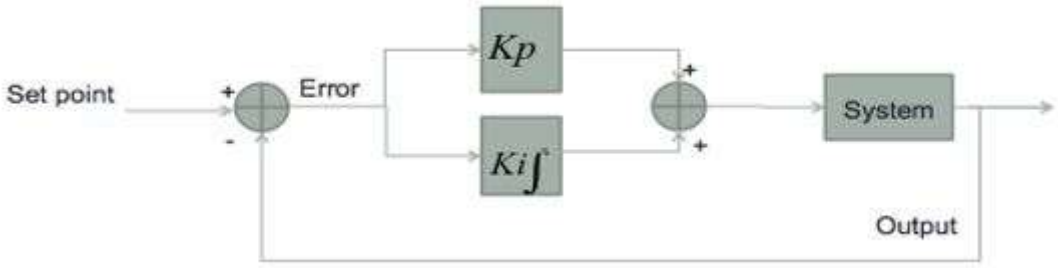

Fig.5.9. Block diagram of PI controller.

The controller output in this case is

$u(t) = K_p \cdot e(t) + K_i \int e(t)\, dt$

Fig. 6.block diagram PI controller an integral error compensation scheme, the output response depends in some manner upon the integral of the actuating signal. This type of compensation is introduced by a using a controller which produces an output signal consisting of two terms, one proportional to the actuating signal and the other proportional to its integral. Such a controller is called proportional plus integral controller or PI controller.

$$\Delta D = \left(K_{p_1} + \frac{K_{i_1}}{S}\right)\left(V_{dc_{ref}} - V_{dc}\right)$$

$$\Delta K_d = \left(K_{p_2} + \frac{K_{i_2}}{S}\right)\left(P_{grid_{ref}} - P_{grid}\right)$$

$$\Delta K_q = \left(K_{p_3} + \frac{K_{i_3}}{S}\right)\left(Q_{grid_{ref}} - Q_{grid}\right)$$

$$\Delta d = \left(K_{p_4} + \frac{K_{i_4}}{S}\right)\left(I_{bat_{ref}} - I_{bat}\right)$$

Small signal representation of the entire system

$$\frac{d\Delta I_{pv}}{dt} = \frac{1 + Z_1}{Z_2 L}\Delta I_{pv} - (1 - \Delta D)\frac{\Delta V_{dc}}{L}$$

$$\frac{d\Delta V_{dc}}{dt} = (1 - \Delta D)\frac{\Delta I_{pv}}{C_1} - \frac{\Delta V_{dc}}{R_1 C_1}$$

$$\frac{d\Delta I_d}{dt} = \omega \Delta I_q - \frac{e_d}{L_{ac}} + \Delta K_d$$

$$\frac{d\Delta I_q}{dt} = \ -\omega \Delta I_d - \frac{e_q}{L_{ac}} + \Delta K_q$$

$$\frac{d\Delta V_t}{dt} = \frac{\Delta I_{bat}}{C_2} - \frac{\Delta V_t}{R_2 C_2}$$

$$\frac{d\Delta I_{bat}}{dt} = \frac{\Delta V_{dc} - \Delta V_t - \Delta I_{bat} R_o - E_o}{L_{dc}} - \frac{\Delta V_{dc}}{L_{dc}}\Delta d$$

$$\frac{d\Delta SOC}{dt} = \frac{\Delta I_{bat}}{C_{bat}}$$

$$\frac{d\Delta D}{dt} = K_{p_1}\left(\frac{1 - \Delta D \Delta I_{pv}}{C_1} - \frac{\Delta V_{dc}}{R_1 C_1}\right) + K_{i_1}\Delta V_{dc}$$

$$\frac{d\Delta K_d}{dt} = \frac{3}{2} e_d K_{p_2}\left(\omega \Delta I_q - \frac{e_d}{L_{ac}} + \frac{\Delta K_d \Delta V_{dc}}{L_{ac}}\right) + \frac{3}{2} e_d K_{i_2}\Delta I_d$$

$$\frac{d\Delta K_q}{dt} = -\frac{3}{2} e_d K_{p_3}\left(-\omega \Delta I_d - \frac{e_q}{L_{ac}} + \frac{\Delta K_q \Delta V_{dc}}{L_{ac}}\right) - \frac{3}{2} e_d K_{i_3}\Delta I_q$$

$$\frac{d\Delta d}{dt} = K_{p_4}\left(\frac{\Delta V_{dc} - \Delta V_t - \Delta I_{bat} R_o - \Delta d \Delta V_{dc} - E_o}{L_{dc}}\right) + K_{i_4}\Delta I_{bat}$$

5.9.2 MATLAB Code For Stability Analysis with Controller

```
clear all;
clc;
%PV Parameters
Vpv=0.1;
Ipv=10.1327;

Rs=0.05;
Rsh=100;
Ns=60;
Np=1;
A=1.3;
k=1.38e-23;
T=298;
Is=2.8393e-10;
q=1.6e-19;
alpha=q/(A*k*T);

% Parameters for Linearization of Ipv
M=(Vpv/Ns)+(Ipv*Rs)/Np;
Z1=Is*alpha*Rs*exp(alpha*M)+Rs/Rsh;
Z2=-(Np/Ns)*alpha*Is*exp(alpha*M)-Np/(Rsh*Ns);

% Dc-Dc Boost
R1=20;
C1=10*10^(-6);
L=1*10^(-3);

%BDC
Lac=.1098*10^(-3);
Cdc=.05*10^(-6);
Ldc=.755*10^(-3);
C2=80;
R2=0.07;
R0=0.0207;
d=0.5;
Q=300;

%Grid
ed=230;
Pgrid=10000;
theta=pi/6;
eq=0;
f=60;
w=2*3.14*f;
```

```
%Equations under Steady State operations
Vdc=sqrt(Vpv*Ipv*R1);
D=1-Vdc/(Ipv*R1);
Id=Pgrid/(1.5*ed);
Idc=(1-D)*Ipv;
Kq=(w*Lac*Id)/Vdc;
Ibat=Idc/(1-d);
Vt=Ibat*R2;
E0 = Vdc*(1 - d)-Vt-(Ibat*R0);
Qgrid=(Pgrid*tan(theta));
Iq=-(2*Qgrid)/(3*ed);
Kd=(((ed/Lac)-w*Iq*Lac)/Vdc);

%PI controller Gain Parameters
Kp1=1.67;
Ki1=4.007;
Kp2=-1.43;
Ki2=-4.003;
Kp3=3.98;
Ki3=7.08;
Kp4=4.06;
Ki4=1.01;


%x1=Ipv; x2=Vdc; x3=Id; x4=Iq; x5=Vt; x6=Ibat;
%x7=SoC;x8=D;x9=kd;x10=kq;x11=d;


syms x1 x2 x3 x4 x5 x6 x7 x8 x9 x10 x11;

f1(x1,x2,x8)=((1+Z1)/(Z2*L))*x1+((D-1)/L)*x2+(Vdc/L)*x8;

f2(x1,x2,x8)=((1-D)/C1)*x1-(Ipv/C1)*x8-x2/(R1*C1);

f3(x2,x4,x9)=w*x4-(ed/Lac)+(Kd*x2)/Lac+(Vdc/Lac)*x9;
f4(x3,x2,x10)=-w*x3-(eq/Lac)+(Kq*x2)/Lac+(Vdc/Lac)*x10;
f5(x5,x6)=(x5/C2)-x6/(R2*C2);
f6(x2,x5,x6,x11)=((x2-x6-x5*R0-E0-Vdc*x11)/Ldc)-(x2*d)/Ldc;
f7(x5)=x5/Q;
f8(x1,x2,x8)=Kp1*x1*(1-D)/C1-(Kp1*Ipv*x8)/C1-
(Kp1*x2)/(R1*C1)+Ki1*x2;
f9(x3,x2,x4,x9)=1.5*ed*Kp2*(w*x4-
ed/Lac+(Kd/Lac)*x2+(Vdc/Lac)*x9)+1.5*ed*Ki2*x3;
f10(x3,x2,x4,x10)=-1.5*ed*Kp3*(-w*x3-
eq/Lac+(Kq/Lac)*x2+(Vdc/Lac)*x10)-1.5*ed*Ki3*x4;
f11(x2,x5,x6,x11)=Kp4*((1-d)*x2-x6-x5*R0-E0-
Vdc*x11)/Ldc+(Ki4*x5);
```

```
a(x1,x2,x3,x4,x5,x6,x7,x8,x9,x10,x11) =
jacobian([f1(x1,x2,x8);f2(x1,x2,x8);f3(x2,x4,x9);f4(x3,x2,x10)
;f5(x5,x6);f6(x2,x5,x6,x11);f7(x5);f8(x1,x2,x8);f9(x3,x2,x4,x9
);f10(x3,x2,x4,x10);f11(x2,x5,x6,x11)],
[x1,x2,x3,x4,x5,x6,x7,x8,x9,x10,x11]);
A=vpa(a,3)

   B=eig(A)
  C=vpa(B,3)
```

5.9.3 Stability Mode Analysis with PI Controller using Eigenvalue

Modes	Eigen Value	State Condition
λ_1	8.9e8	Unstable
λ_2	2.33	Unstable
λ_3	1.78	Unstable
λ_4	0.21	Unstable
λ_5	-9.46e-47	Stable
λ_6	-0.20	Stable
λ_7	-2.8	Stable
λ_8	-553.5	Stable
λ_9	-3.84e5	Stable
λ_{10}	-1.70e6	Stable
λ_{11}	-3.19e8	Stable

Gain Parameters	Values
K_{p_1}	1.3
K_{i_1}	-2.75
K_{p_2}	-3.25
K_{i_2}	6.50
K_{p_3}	-2.2
K_{i_3}	5.30
K_{p_4}	0.75
K_{i_4}	-1.15

5.9.4 Participation Factor

Today it is known two different approaches to the participation factor of state variable in mode: the approach of scientists Perez-Arriaga and Verghese, and approach of group of scientists led by E.H. Abed. Before we consider these approaches let's briefly overview of the history of participation factor problematics.

The power system under study consists of a number of *N* synchronous machines connected by a large number of connections. In the linear approximation, the description of this power system can be presented with the system of differential equations:

$\dot{\mathbf{x}} = \mathbf{A}\mathbf{x}$, (1)

where **x** – column vector of state variables, **A** – characteristic matrix of differential equations system by which power system is described in the linear approximation. In the case of power system description matrix A is real, that is,

A* = **A**. In general, the matrix A has *N* different eigenvalues, some of which are a complex conjugate:

$\lambda i = \sigma i \pm j\omega i$, (2) where σi – real part of eigenvalue which characterizes state stability margin of power system, ωi – imaginary part of eigenvalue which determines fluctuation frequency of power system mode. By stability margin we shall basically mean real part module of eigenvalue. Left and right eigenvectors that correspond to eigenvalue λi are defined by expressions:

$$\mathbf{A}\mathbf{r}_i = \lambda_i \mathbf{r}_i$$
$$\mathbf{l}_i \mathbf{A} = \mathbf{l}_i \lambda_i$$

How does one generally proceed in a small-signal analysis study?

1. Compute eigenvalues and eigenvectors for a certain operating condition.

3. Identify right pk and left qk eigenvectors for mode k.

a. Identify “groups” of generators based on mode shape using

pk (use the angles of the elements of pk corresponding to the speed deviation states).

b. For each group, identify the speed deviation states (and thus the generators) most heavily participating (influencing) the mode.

5.9.5 MATLAB Code For Stability Analysis with Controller using Participation Factor

```
clc;

clear all;


 a=[

 -1.36e6,     -22.2,         0,         0,         0,         0, 0,
4500.0,         0,         0,         0;
  2222.0,  -5000.0,         0,         0,         0,         0, 0, -
1.01e6,         0,         0,         0;
       0,   4.24e9,         0,    377.0,         0,         0, 0,
0,    4.1e4,         0,         0;
       0,   2433.0,  -377.0,         0,         0,         0, 0,
0,         0,    4.1e4,         0;
       0,         0,         0,         0,   0.0125,   -0.179, 0,
0,         0,         0,         0;
```

```
       0,    662.0,        0,        0,   -27.4, -1322.0, 0,
0,       0,        0, -5966.0;
       0,        0,        0,        0, 0.00333,        0, 0,
0,       0,        0,        0;
  3711.0,  -8355.0,        0,        0,        0,        0, 0, -
1.69e6,        0,        0,        0;
       0, -2.09e12, -1388.0, -1.86e5,        0,        0, 0,
0, -2.02e7,        0,        0;
       0,  -3.33e6,  5.17e5, -2444.0,        0,        0, 0,
0,       0, -5.63e7,        0;
       0,   2699.0,        0,        0,  -110.0, -5388.0, 0,
0,       0,        0, -2.42e4];


  [P,H]=eig(a);
  QT=inv(P);
  Q=QT';
j=1;
% j is index on columns (modes)
% i is index on rows (states)
while j<12,
i=1;
while i<12,
pf(i,j)=(Q(i,j)*P(i,j));
i=i+1;
end
j=j+1;
end
pf
```

5.9.6 Stability Mode Analysis with PI Controller using Participation Factor

Modes	Eigen Value	State Condition
λ_1	0.213	Unstable
λ_2	-1.16e-50	Stable
λ_3	-0.2	Stable
λ_4	-1.78	Stable
λ_5	-2.39	Stable
λ_6	-2.8	Stable
λ_7	-3.1e4	Stable
λ_8	-6.0e5	Stable
λ_9	-2.54e6	Stable
λ_{10}	-2.48e7	Stable
λ_{11}	-6.89e7	Stable

Gain Parameters	Values
K_{p_1}	1.67
K_{i_1}	4.007
K_{p_2}	-1.43
K_{i_2}	-4.003
K_{p_3}	3.98
K_{i_3}	7.08
K_{p_4}	4.06
K_{i_4}	1.01

```
pf =

         0    0.0000   -0.0000    0.0001    0.9999    0.0000
         0   -0.0000   -0.0000    0.0029    0.0000    0.0000
         0   -0.0000   -0.0000    0.0000   -0.0000    0.0000
         0   -0.0000    0.0000    0.0000    0.0000    0.0000
         0    0.0000    0.0000    0.0000   -0.0000    0.0000
         0    0.0000    0.0000   -0.0000    0.0000    0.0520
    1.0000         0         0         0         0         0
         0    0.0000    0.0000    0.9969    0.0001    0.0000
         0   -0.0000    1.0000    0.0000    0.0000   -0.0000
         0    1.0000   -0.0000   -0.0000    0.0000    0.0000
         0    0.0000    0.0000    0.0000   -0.0000    0.9480
```

5.9.7 Eigen Root-locus With Controller

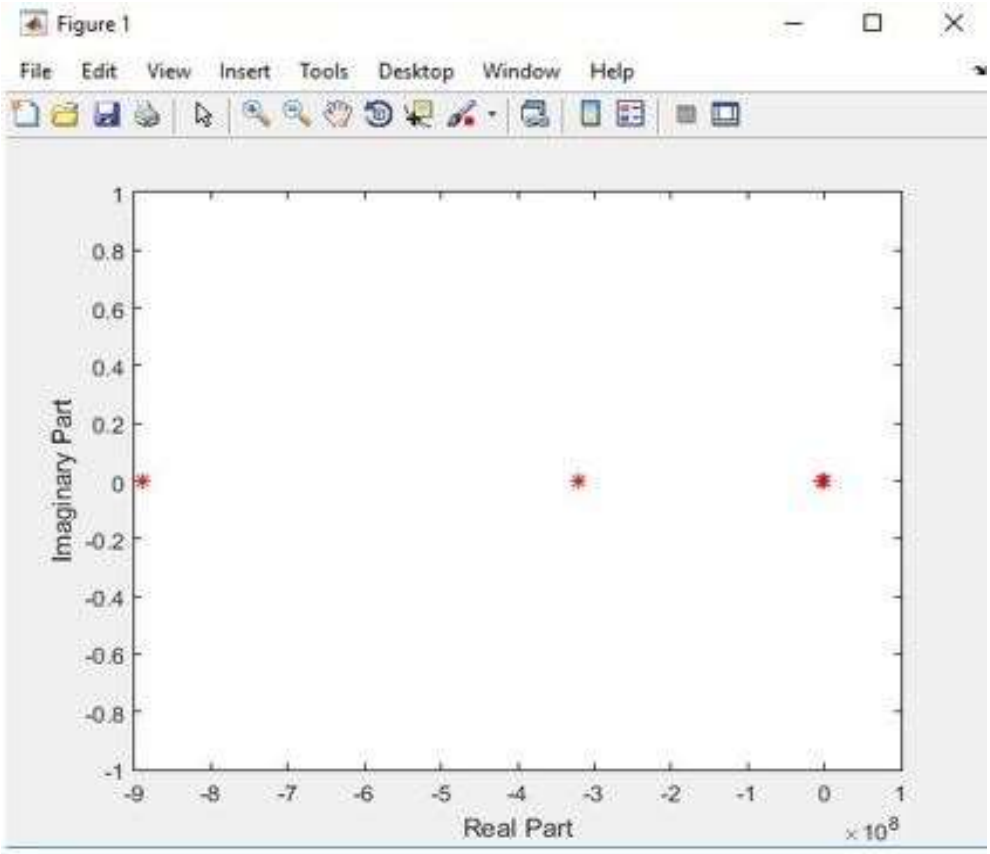

With Controller

Chapter 6

Conclusion

This research work basically focuses on the mathematical modelling of grid connected PV+BESS system & stability analysis with the help of small signal stability introducing eigenvalue analysis. Now it is clear that alternative source of energy based electric energy generation may ben explored to continue generation of electrical power to meet the demand.

Although, among the renewable energy sources, the solar energy is considered one of the most

popular because of the availability of free light energy from sun. .Due to fluctuation of weather (solar irradiance & temperature) how the system's stability will be is discussed in this research work. Solar irradiance & temperature variation is considered as small signal disturbances in case of PV generation..The challenge of using PV is that it can be easily used in stand-alone way

but difficulties arise if it is connected to grid. Therefore, in this thesis, Voltage Source Inverter (VSI) generator has been studied with its dynamic model first. After that, modeling is done with

the connection to grid. The complete grid connected PV with BESS has been designed for open loop and closed loop PI controller. Finally the stability of the system has been analysed using Eigenvalue. Special attention has been given to the control strategies of PV+BESS feed to grid.

It should be mentioned that the impact of PV power on power system small signal stability is studied elaborately. Furthermore, the mathematical treatment of the linearization of the non-linear equations describing a power system and of the relation

between the eigenvalues and the time domain was given. This work also includes participation factor for identification of state mode. The simulation results is carried out using Matlab software. A critical assessment of small signal stability analysis is carried out for different scenarios such as variation of parameters of PV pannel, implementation of closed loop PI controller without optimization. More specifically, it was found that stability of the PV+BESS system connected to grid using conventional PI controller without optimization depends to a large extent on thetuning of the proportional-integral controllers and on having good knowledge of the systemparameters. It should be noticed the tuning of PI controller gains manually are tedious work. Achange in operating scenarios or system topology may require a re-tuning of the PI controllers gains. controller. The obtained result is compared with the PI controller performance without optimization.

Implementation of the genetic algorithm optimization of closed loop PI Controller for far better performance may be studied as future work. The transient behavior of the grid connected PV+BESS under proposed controller may be studied under large disturbance

In the last, it can be expected that this work may be helpful in feeding the grid with wind generated power for a stable operation.

References

[1] Ding, Fei, et al. "Modeling and simulation of grid-connected hybrid photovoltaic/battery distributed generation system." *Electricity Distribution (CICED), 2010 China International Conference on*. IEEE, 2010.

[2] Mahmud, Md Apel, H. R. Pota, and M. J. Hossain. "Dynamic stability of three-phase grid-connected photovoltaic system using zero dynamic design approach." *IEEE Journal of Photovoltaics* 2.4 (2012): 564-571.

[3] Wang, Bingjie. "Peak shaving and energy management for grid-connected pv systems integrated with battery storage." (2015).

[4] Kim, Il-Song. "Robust maximum power point tracker using sliding mode controller for the three-phase grid-connected photovoltaic system." *Solar Energy* 81.3 (2007): 405-414.

[5] Qi, J. I. A., et al. "Small-signal stability analysis of photovoltaic generation connected to weak AC grid." *Journal of Modern Power Systems and Clean Energy* (2018): 1-14.

[6] Smitha, K., et al. "Steady state analysis of PID controlled boost converter using state space averaging technique." (2015): 100-110.

[7] Benkhelil, E., and A. Gherbi. "Modeling and simulation of grid-connected photovoltaic generation system." *Revue des Energies Renouvelables SIENR* 12 (2012): 295-306.

[8] Rodriguez, Cuauhtemoc, and G. A. J. Amaratunga. "Dynamic stability of grid-connected photovoltaic systems." *Power Engineering Society General Meeting, 2004. IEEE*. IEEE, 2004.

[9] VijayRaol, M., M. Parahanth Reddy, and B. Sreedhar. "Voltage-Oriented Control of A Grid Connected PV System By Modified MPPT Algorithm." *International Journal of Ressearch, JNTYH, AP, India* (2013).

[10] Mahmud, M. A., M. J. Hossain, and H. R. Pota. "Dynamic stability analysis of photovoltaic systems using Lyapunov functions." *48th Annual Conference of Australian Solar Society. Canberra, Australia*. 2010.

[11] Daud, M. Zalani, et al. "Performance evaluation of grid-connected photovoltaic system with battery energy storage." *Power and Energy (PECon), 2012 IEEE International Conference on*. IEEE, 2012.

[**12**] Wang, B., M. Zarghami, and M. Vaziri. "Energy management and peak-shaving in grid-connected photovoltaic systems integrated with battery storage." *North American Power Symposium (NAPS), 2016*. IEEE, 2016.

[13] Seo, Hun-Chul, and Chul-Hwan Kim. "Analysis of Stability of PV System using the Eigenvalue according to the Frequency Variation and Requirements of Frequency Protection." *Journal of Electrical Engineering and Technology* 7.4 (2012): 480-485.

[14] Rajyaguru, Vipul C. "Design and Simulation of Grid Connected PV System.“

[15] Breitenstein, Otwin. "An alternative one-diode model for illuminated solar cells." *Energy Procedia* 55 (2014): 30-37.

[16] Jeyraj Selvaraj, Nasrudin A. Rahim. "Multilevel Inverter For Grid-Connected PV System

Employing Digital PI Controller." *IEEE Transactions On Industrial Electronics*, Vol. 56, No. 1, January 2009.

[17] Pallavi Appaso Arbune, Dr. Asha Gaikwad. "Comparative Study of Three level and Five level Inverter." *International Journal of Advanced Research in Electrical, Electronics and Instrumentation Engineering* Vol. 5, Issue 2, February 2016.

[18] Utsav P. Yagnik, Mehul D. Solanki. "Comparison of L, LC & LCL filter for grid connected converter." *International Conference on Trends in Electronics and Informatics* ICEI 2017

[19] Reena Ingudam, Roshan Nayak, ”Modelling and Performance Analysis of DC-DC Converters for PV Grid Connected System,” *International Journal of Science, Engineering and Technology Research (IJSETR),* Volume 4, Issue 5,pp. 1382-1383,1387 May 2015 ISSN 2274-7798

[20] Ned Mohan. Power Electronics Converters Applications and Design,*Wiley* Chapter 10.5,Pg.323

[21] K.W.E.Cheng, “Classical switched mode and resonant power converters”, *Hong Kong Polytechnic University*, ISBN 962-367-364-7

[22] Smitha K, Priyanka G Aryar, Renuka Bijlwan, Sachin Angadi,” Steady State Analysis of PID Controlled Boost Converter using State Space Averaging Technique,” *Multidisciplinary Journal of Research in Engineering and Technology (MJRET),* Pg.100-110,2015